

**HYBRID FLEXIBLE SOLAR PHOTOVOLTAIC AND ELECTRIC DOUBLE-
LAYER CAPACITOR FOR WEARABLE DEVICE APPLICATION**

LEONG WAI LUN

**A project report submitted in partial fulfilment of the
requirements for the award of Bachelor of Engineering
(Honours) Mechanical Engineering**

**Lee Kong Chian Faculty of Engineering and Science
Universiti Tunku Abdul Rahman**

April 2021

DECLARATION

I hereby declare that this project report is based on my original work except for citations and quotations which have been duly acknowledged. I also declare that it has not been previously and concurrently submitted for any other degree or award at UTAR or other institutions.

Signature :

Name : LEONG WAI LUNID No. : 1605138Date : 8/5/2021

APPROVAL FOR SUBMISSION

I certify that this project report entitled “**HYBRID FLEXIBLE SOLAR PV AND ELECTRIC DOUBLE-LAYER CAPACITOR FOR WEARABLE DEVICE APPLICATION**” was prepared by **LEONG WAI LUN** has met the required standard for submission in partial fulfilment of the requirements for the award of Bachelor of Engineering (Honours) Mechanical Engineering at Universiti Tunku Abdul Rahman.

Approved by,

Signature :



Supervisor :

Dr. Jun Hieng Kiat

Date :

8/5/2021

The copyright of this report belongs to the author under the terms of the copyright Act 1987 as qualified by Intellectual Property Policy of Universiti Tunku Abdul Rahman. Due acknowledgement shall always be made of the use of any material contained in, or derived from, this report.

© 2021, Leong Wai Lun. All right reserved.

ACKNOWLEDGEMENTS

I would like to thank everyone who had contributed to the successful completion of this project. I would like to express my gratitude to my research supervisor, Dr. Jun Hieng Kiat for his invaluable advice, guidance and his enormous patience throughout the development of the research.

In addition, I would also like to express my gratitude to my loving parents and friends who had helped and given me encouragement with this limited time frame.

ABSTRACT

A standalone energy generating and storing hybrid system involving flexible solar photovoltaics (Solar PV) and flexible silver coated textile coated with activated carbon electric double layer capacitor (EDLC) is built. The use of 3D porous textile structure as electrodes allows more activated carbon to stick onto the surface of the electrodes and provide a bigger surface area to store charges. The silver coated textile based EDLC in this study shows areal capacitance of 2.89 mFcm^{-2} and specific capacitance of 71.32 Fkg^{-1} . The power density of the EDLC is 0.01316 Wcm^{-2} and energy density is $0.01247 \text{ Whcm}^{-2}$. The EDLC shows prolonged cycling stability, which is 100% retention rate after 100 cycles. Furthermore, when the EDLC is paired with flexible solar PV to form a standalone power generating and storing device, it achieves overall conversion efficiency of 2.2%. The 5 cm^2 of EDLC able to discharge continuously to power up wearable electronics for 30 minutes with 5 seconds of charging under the sun, this shows that such system can power up wearable electronics at outdoor environment without a battery. The hybrid system is lightweight, biocompatible and flexible. It is highly flexible that it can be bent 180 degrees or rolled without losing its properties. Our study offers a new kind of high mobility standalone power generation and storing device for wearable technologies.

TABLE OF CONTENTS

DECLARATION	i
APPROVAL FOR SUBMISSION	ii
ACKNOWLEDGEMENTS	iv
ABSTRACT	v
TABLE OF CONTENTS	vi
LIST OF TABLES	viii
LIST OF FIGURES	ix
LIST OF SYMBOLS / ABBREVIATIONS	xii
LIST OF APPENDICES	xiii

CHAPTER

1	INTRODUCTION	1
	1.1 General Introduction	1
	1.2 Importance of the Study	2
	1.3 Problem Statement	3
	1.4 Aim and Objectives	3
	1.5 Scope and Limitation of the Study	4
	1.6 Contribution of the Study	4
	1.7 Outline of the report	5
2	LITERATURE REVIEW	6
	2.1 Introduction	6
	2.2 Flexible Solar PV	6
	2.3 Recent development of flexible Solar PV	9
	2.4 Supercapacitor	10
	2.5 Electrodes and Electrolyte used for the EDLC	12
	2.6 Architecture of flexible EDLC	13
	2.7 Performance measurement of the hybrid device	20
	2.8 Recent development of the hybrid device	21
	2.9 Summary	22
3	METHODOLOGY AND WORK PLAN	23

3.1	Introduction	23
3.2	Methodology	23
3.2.1	Flexible solar PV	23
3.2.2	Flexible fabric based EDLC	24
3.3	Characterisations	27
3.4	Work Plan	32
3.5	Full Gantt Chart	33
3.6	Summary	34
4	RESULTS AND DISCUSSION	35
4.1	Conductivity of gel electrolyte	35
4.2	Potential windows of the electrolyte	38
4.3	Physical Properties of the EDLC	40
4.4	Cyclic Voltammetry (CV) of EDLCs	40
4.5	GCD test on the EDLCs	46
4.6	Output of flexible solar PV	47
4.7	Performance of the hybrid device	49
4.8	Summary	50
5	CONCLUSIONS AND RECOMMENDATIONS	52
5.1	Conclusions	52
5.2	Recommendations for future work	52
	REFERENCES	54
	APPENDICES	60

LIST OF TABLES

Table 3.1:	Gantt chart of the experiment works	32
Table 3.2:	Gantt Chart of the full final year project	33
Table 4.1:	Measurement of conductivity of different samples.	37

LIST OF FIGURES

Figure 2.1:	The working principle of DSSC.	7
Figure 2.2:	Figure shows left 1 is PSC with mesoporous structure, left 2 is PSC with HTL-free mesoporous structure, right 1 is PSC with p-i-n planar structure, right 2 is PSC with n-i-p planar structure.	8
Figure 2.3:	The structure of organic solar cell	9
Figure 2.4:	Illustration of charging and discharging mechanism of EDLC.	11
Figure 2.5:	The illustration of charging-discharge mechanism of pseudocapacitor.	12
Figure 2.6	Figure of various type of build for fiber-like flexible supercapacitors.	14
Figure 2.7	Figure of paper-like FSCs is shown in part (a) of the figure, free-standing paper-like FEs is shown in part (b) of the figure and flexible substrate supported FEs is shown in part (c) of the figure	15
Figure 2.8	Structure of PANI coated CNTs electrode.	16
Figure 2.9	(a) Figure shows bending of flexible MnO ₂ electrode which consists of large surface area (b) Figure shows structure of the EDLC which consists of separator and MnO ₂ electrodes. (c) Set-up used for the actual demonstration of flexible MnO ₂ electrodes.(d) The structure of flexible MnO ₂ supercapacitor.	17
Figure 2.10	(a) Figure shows cellulose fibers is wrapped by SWNTs to form individual cotton fibrils, and stacked fibrils to form 3D porous structure. (b), (c) By dipping textiles into an aqueous SWNT ink and dried by oven under 120 °C for 10 min to make conductive fibre	19
Figure 2.11	Steps to fabricate GFSC electrodes to assemble into complete GFSC fill cell.	20
Figure 3.1	Photo of flexible solar PV from WarmSpace, which use 3layers amorphous silicon solar cell and packed with ETFE technology.	24
Figure 3.2.	Picture illustrates the mixing process of activated carbon coating (right) and PVA gel (left).	25

Figure 3.3:	Photo of activated carbon coating applied on silver coated clothing (2nd row) and aluminium sheet (1st row) for the 1st time.	25
Figure 3.4:	Liquid form of H ₃ PO ₄ gel electrolyte after 5 hours of mixing.	26
Figure 3.5:	Figure illustrates fabricated EDLCs made of silver cloth (left) and aluminium sheet (right).	27
Figure 3.6:	Measurement on flexible solar PV using multimeter.	28
Figure 3.7:	Figure shows EIS conducted on PVA gel electrolyte measured with ZIVELAB potentiostat.	29
Figure 3.8:	Photo shows the method used to charge EDLCs with solar PV, where the multimeter is parallel to the circuit of solar PV and EDLC to measure the voltage provided by the solar PV to EDLC.	30
Figure 3.9:	Photo shows the method used to measure the discharge EDLCs using multimeter.	30
Figure 3.10:	Photo shows the circuit diagram used to measure the performance of EDLC and Solar PV, where C1 and C2 is the silver coated textile EDLC, and the DC Voltmeter is the multimeter, voltage source is the solar PV. The left shows the circuit diagram during charging of the EDLC and the right shows the circuit diagram during discharging of the EDLC.	31
Figure 4.1:	Potentiostatic EIS static set-up setting to measure the conductivity of the electrolyte.	36
Figure 4.2:	Nyquist plot of the electrolyte, plot with Potentiostat EIS shows the bulk resistance of sample 1 is 64.278 k Ω .	36
Figure 4.3:	Settings of Linear Sweep Voltammetry analysis.	39
Figure 4.4:	Linear Sweep Voltammetry of the electrolyte. Where the graph is flat from -1.5V to 1.5V, which represents the potential windows of the electrolyte.	39
Figure 4.5:	Silver coated textile EDLC is rolled into round shape (Left 1) and bent 90 degrees (Left 2), the shapes of the EDLC still retains without any damage (Left 3).	40
Figure 4.6:	The result of CV analysis on silver coated textile EDLC sample 1 (Orange color line), silver coated textile EDLC	

	sample 2 (grey color line) and aluminium sheet EDLC sample (blue line).	42
Figure 4.7:	The settings parameter for the CV test.	42
Figure 4.8:	Graph plot using OriginPro to calculate the area under the curve.	43
Figure 4.9:	Photo illustrates Zview analyse the EIS graph for ESR.	46
Figure 4.10:	Setting for GCD test.	47
Figure 4.11:	GCD testing on silver cloth EDLC (sample 1).	47
Figure 4.12:	Performance of Solar PV under high light and low light condition	48
Figure 4.13:	Graph of output of voltage over time for silver coated textile EDLC	50

LIST OF SYMBOLS / ABBREVIATIONS

η	Efficiency of solar cells
P_{max}	Solar PV maximum power output, W
A	Surface area of the solar PV, m^2
E_{tot}	Total irradiance that the solar PV is exposed, Wm^{-2}
T	Thickness of the electrolyte, s
A	Area of the electrolyte measured, m^2
R_b	Bulk resistance of the electrolyte, Ω
C_A	Specific capacitance of the EDLC, F
$\int I dV$	Area under the CV graph obtained, A
A	Area of active element, cm^2
ΔV	Electrochemical potential windows of the electrolyte, V
V	Scanning rate used to get the CV curve, $mV s^{-1}$
C_p	Specific capacitance, F
m	Mass of the active element, kg
E	Energy density, Wm^{-2}
P_A	Power density, W/m^2
ESR	Equivalent series resistance of the supercapacitor, Ω
I_{dis}	Current discharged by the EDLC, A
$\int v dt$	Voltage during discharge, V
S	Active light collection area of the solar PV, m^2
T	Time the light illuminates on the solar PV, s
P	Power density of the light receives by the solar PV, W
EDLC	Electric Double Layer Capacitor
PV	Photovoltaic
GCD	Galvanostatic Charge-Discharge
LSV	Linear Sweep Voltammetry
EIS	Electrochemical Impedance Spectroscopy
Cc/cv	Constant charge / constant voltage
CV	Cyclic Voltammetry

LIST OF APPENDICES

APPENDIX A: Circular modelling of nyquist plot data using ZMAN Zive	60
APPENDIX B: GCD Graph of EDLCs	62
APPENDIX C: CV Graph of EDLCs	64
APPENDIX D: Nyquist graph fitting of EDLCs using Zview.	65
APPENDIX E: Calculations	67

CHAPTER 1

INTRODUCTION

1.1 General Introduction

With the recent developments of GPS systems, electronic chip, sensors, mobile phones and the internet, the demand for wearable technologies have been growing, according to Allied Market Research, that market values of USD 57.623 billion is expected to be reached by the global market size of wearable technologies (Allied Market Research 2019). The wearable technologies are defined as technologies that holds multiple items, including items that use electronics, items that use functional materials and items that use mechanical technologies, the technologies must not be supported by hands when using and it can be wear on the body (Dunne, 2015). These devices will have basic computing functions and often equipped with a sensor to perform measurement in real time, and can be found in wide ranges of products, which included smart watches, fitness trackers, implantable, smart glasses, smart belts, head mounted displays and smart jewellery.

However, wearable technologies faced a few challenges which include deprived battery life and lack of waterproofing charging method which impact performance and user experiences of the wearable devices (Kalia, 2020). Hence, recent developments have been focused on harvesting energy sources from ambient environment to make the wearable technologies self-sustaining. Sources such as light, thermal, mechanic and electromagnetic radiation (ER) are used to generate energy on wearable technologies from ambient environment. Among all the sources, light energy is the easiest source of energy to harvest.

To harvest solar energy on wearable technologies, solar photovoltaic system (Solar PV) is needed to convert the light energy to electricity. Solar PV functions by accepting photons from sunlight which will push the extra electron inside the doped material, which is usually n-doped silicon to flow in the wiring connected to the solar pv and produce current. However, the solar PV needed to be able to fit into the wearable technologies so that people will be able to carry it easily. Hence, flexible Solar PV, which has properties of light in weight, thin in size, easy processability, high transportability, high flexibility, can be produced by roll-to-roll procedure, can be joined to curve surface, is preferable.

However, as solar energy is intermittent in nature, so media of storing energy is required to stabilize the output of the flexible solar PV and store the input of energy more efficiently (Ng et al., 2015). The energy storing device can be supercapacitors, lithium-ion batteries, zinc-ion batteries, however, as the energy provided by solar PV is highly unstable and storing devices only required to provide continuous energy when light energy is not accessible, so supercapacitors is more preferable, as batteries will be less reliable for long term use, and might cause inflammation and volumetric modulation during rapid charge-discharge cycle, slower to be charged up and less environmental friendly compare to supercapacitors (Chen, Paul, & Dai 2017).

Supercapacitors functions by positively charging one side of electrode and negatively charging the other side of the electrode to separate the charges on the dielectric material in between the electrode. Then, where there is no charge on both electrodes, the charges will be discharged through the wiring circuit and provide electricity. There is a few types of supercapacitors in the market today, which are electrostatic double layer capacitors (EDLC), which storage of electricity is by ion absorption, pseudo-capacitors (PC), which charges are stored by fast surface redox reactions and hybrid capacitors (HC), which combined the battery together with the EDLC/PC.

However, most of the market available EDLCs are not flexible, bulky, energy density is low, faces electrical connection issues, hard to be wore on our hands and uncomfortable in handling (Zhai et al., 2016). Hence, a new type of EDLC which is made of comfortable, lightweight and flexible material is developed, which is textile based EDLC.

1.2 Importance of the Study

The result of this present study may lay the foundation for wearable technology to integrate hybrid flexible solar PV and EDLC circuit as the main energy sources for the system, it is important for several reasons, which are:

1. To build self-powered lightweight and flexible material that is able to generate and store energy outdoor to power up wearable electronics.
2. To solve energy storage issues that are faced by smart textile industry and develop the next generation of smart textile.

3. To develop a lightweight, high capacitance EDLC with the commercially available fabrics to speed up the commercialization of flexible EDLC.

1.3 Problem Statement

Problem statement for the current study of hybrid flexible solar PV with EDLC are summarized as below:

Silver coated textile has been on the market for a long time and the high electrical conductivity ($6.30 \times 10^7 \frac{S}{m}$ at 20°C) of such fabric is suitable to construct EDLC electrode because higher electrical conductivity will improve the utilization of electrical energy stored in EDLC and allow the EDLC to discharge and charge with higher current density. Furthermore, the 3D porous structure of textile material can adhere more activated carbon coating on it with cheap and reliable coating methods compare to pure silver. Hence, the performance of EDLC that use silver coated fabric coated with activated carbon is needed to be investigated.

When the lightweight, highly flexible EDLC is paired with lightweight, highly flexible solar PV, they have the potential as lightweight and flexible energy generator and storage system for wearable device. However, the efficiency and performance of such system is still unclear and there is little research being carried out to study the performance of such system. Hence, it is of interest to perform performance evaluation and testing on such system.

1.4 Aim and Objectives

The main aim of this study is to presents textile based EDLC that can integrate with flexible solar PV that can power up wearable devices. The specific objectives of this research is to:

1. To investigate the performance of solid-state EDLC made with commercially available silver coated textile coated with activated carbon paste and PVA gel.
2. To develop a self-sustainable, lightweight and flexible energy generating and storage system with flexible EDLC.
3. To evaluate the overall performance and efficiency of the hybrid flexible solar PV and EDLC for wearable device application.

1.5 Scope and Limitation of the Study

The scope of study for this project is to investigate the performance and development of solid-state textile based EDLC and hybrid of such EDLC with flexible solar PV.

There are a few limitations for this study. First, the time limitation of this study limited the amount of work that can be done, hence, only the flexible EDLC will be built from scratch while the Solar PV is purchased from the market for the study.

Furthermore, due to budget limitation, the solar PV is not high efficiency and the power generated by such solar PV is not that great compare to the solar PV on the market. Then, there will be no electronics or sensors equipped with such hybrid system to test for feasibility of such system in real life as the electronic components required for testing is expensive.

However, the power output of the complete hybrid system will be collected and used to evaluate the sensors and electronics that can be mounted on the wearable technologies and the performance of hybrid flexible solar PV with flexible EDLC to power up electronics during real life application will be evaluated.

Another limitation is the lack of instruments and techniques available to collect the data. In this experiment, the apparatus available to obtain the data is limited as the whole experiment is conducted during movement control period, where access to school facilities is limited. Most of the apparatus and methods used by other studies are not available for this research. So, some of the calculation might be affected by the inaccuracy of the data.

1.6 Contribution of the Study

This study's finding will bring contribution to the society as silver coated textile is available to the society for a long period of time. The use of such textile for energy storing will provide a new way to power up the wearable device. The high mobility of the hybrid study in this system will be able to replace the bulkiness of energy storing system in current technology. Furthermore, the investigation might also reveal important information about textile EDLC that many researchers may not explore before.

1.7 Outline of the report

This report consists of several parts, in the first part, the objective and importance of this study is introduced, this is to ensure that the reader understands the importance of the topic in this research. After that, various literatures are reviewed to gain insight about the topic, this is to ensure the reader understand the background study of this research. Then, methodology of this topic is explained. The experiment and research procedures carried out to test the result is explained. The result of the experiment and discussion about the result is explained in the next section. Finally, the conclusion obtained from the experiment is reported in the final section, the recommendation to obtain better results is also explained here.

CHAPTER 2

LITERATURE REVIEW

2.1 Introduction

The literature review of this study includes several things. First, the working mechanism, build and market of flexible solar PV and EDLC. Then, the performance of various textile EDLCs, which consists of different kinds of textile electrodes and electrolyte. After that, the performance of hybrid flexible solar PV with EDLC system.

2.2 Flexible Solar PV

Flexible solar PV cell consists of a set of photoactive layer, cathode and anode. Although there are many recently developed technologies in flexible solar cell, the most mature technology for such cell is the use of amorphous silicon in developing thin film flexible solar PV.

Amorphous silicon solar PV is fabricated by allowing a few layers of thin film of silicon to be deposited onto the substrate such as plastic, silver or copper. The multilayer of thin film of silicon deposited on the substrate is made differently, where each layer is doped differently to absorb light consists of different spectrum, such architecture allows higher efficiency converting light under low light intensity and the wider spectrum of light is able to be converted to electricity, and the thin film also allow the cell to be flexible ("3 Generations of Solar Cells: Solar Facts and Advice", 2020). Furthermore, such technology also established high productivity and low-cost fabrication methods since 1994, (Sakurai & Sakai, 1999), so it is a mature technology for mass commercialization. Such fabrication can produce layer of non-crystallize silicon that is very thin and can be flex easily with a greater degree, and the whole process of fabrication uses lesser silicon and releases a smaller amount of toxic materials compare to monocrystalline and polycrystalline silicon cell. Although it has long achieved maturity, it still faces issue with lower efficiency currently as compare to monocrystalline and polycrystalline solar cells.

The recent development of flexible solar cell consists of 3 main groups which are flexible dye-sensitized solar cell, perovskite solar cell and organic solar cell. (Hashemi, Ramakrishna, & Aberle, 2020). Flexible dye-sensitized solar cell (DSSC) is made up of conductive and clear substrate, sensitizer which acts as dye, working

electrode, counter electrode and redox-mediator which acts as the electrolyte. The working principle is that during light exposure, the sensitizer, where the Dye is excited and oxidized by the working electrode, TiO_2 , which causes the release of the electron to the conductive substrate and produces current in the circuit, then the dye will regenerate and accept the electron released from the counter electrode side and complete the circuit, as shown in Figure 2.1. DSSC have the benefits of effortless manufacture, low poisonousness, low-cost fabrication method and simple preparation methodology. However, with current research progress, the main material of DSSC, which is Ru(II) still suffer from the higher cost of materials used, and DSSC also possess lower reliability than other types of solar cell. Furthermore, the highest efficiency that the solar cell provided is only $\sim 12\%$, which is still less marketable than the other type of flexible solar cell (Sharma, Sharma & Sharma, 2018).

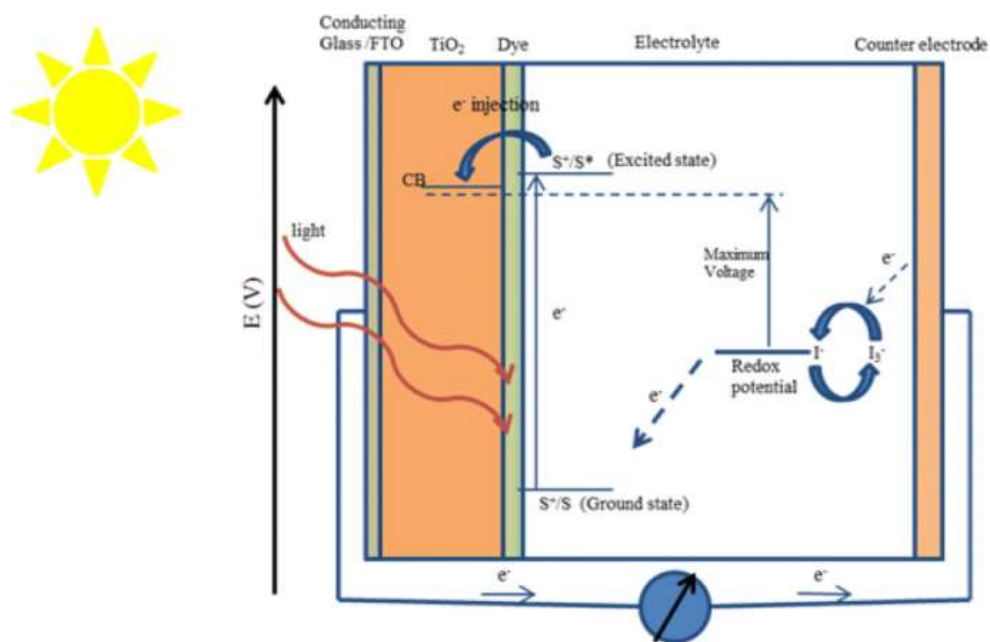


Figure 2.1: The working principle of DSSC (Sharma, Sharma & Sharma, 2018).

The perovskite solar cell (PSC) is the solar cell that uses compound with perovskite structure as the main role of photoelectric conversion and light absorption material. It can be divided into 2 categories which are planar structure and mesoscopic structure as shown in Figure 2.2. The structure of mesoporous structure, which consists of a conductive and clear layer cathode (FTO), a n-type layer (TiO_2) for transportation of the electrons, a mesoporous meta oxide layer filled with perovskite, tailed by

perovskite layer, then, it has hole transporting layer (HTL) for charge transportation purpose, and a metal anode (Ag or Au), while HTL-free mesoporous structure will not possess HTL in the structure and metal anode in the structure, but replaced with carbon electrodes. The mesoporous layer can assist in helping the cell to achieve higher efficiency and less hysteresis, but it will cause higher difficulty in manufacture as the process to deposit perovskite will be harder. The planar structure of perovskite solar cell is built from FTO, perovskite layer, metal anode and compact n-type layer with HTL for n-i-p planar structure and compact p-type layer with electron transporting layer (ETL) for p-i-n planar structure as shown in Figure 2.2. Overall, PSC has several benefits such as outstanding carrier mobility, low-cost, large absorption coefficient and high efficiency, which is up to 22.1% (Fu et al., 2018). However, the PSC degrades fast and will have issue in long term constancy in efficiency due to the stability issue of the perovskite material.

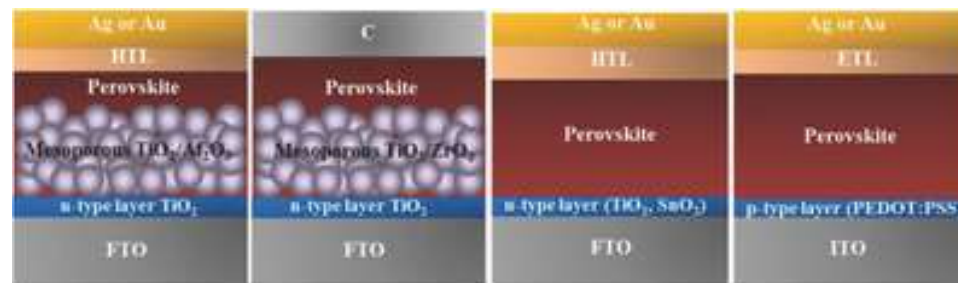


Figure 2.2: Figure shows left 1 is PSC with mesoporous structure, left 2 is PSC with HTL-free mesoporous structure, right 1 is PSC with p-i-n planar structure, right 2 is PSC with n-i-p planar structure (Fu et al., 2018).

Organic solar cell (OSC), unlike the other cells, uses organic electronics and is environment friendly, which is made up of a n-type electron acceptor layer and p-type electron donor layer along with ETL and HTL, which is for charge transport purpose, then it is packed in between a cathode and an anode layer as shown in Figure 2.3. The general mechanism of the organic solar cell is when the light hits onto the organic semiconductor, the semiconductor splits into electron and hole pairs, and transform into free charge which will transport through some materials to be collected by the electrodes that is connected to the external circuit, thus creating current in circuit. The organic solar cell has the benefits of having simple manufacturing and production technique, can be integrated with other technologies and the material is made of

abundant and low-cost earth materials, which can achieve ~10% of efficiency (Vivek, 2014). Recent technologies and architecture also uses “all-polymer solar cells”, which consisted of an assembly of the complete polymeric organic solar cell can reach efficiency up to 12% (Hashemi, Ramakrishna, & Aberle, 2020). However, OSC still faces a few disadvantages that hinder its mass commercialization which including low lifetime and less reliability.

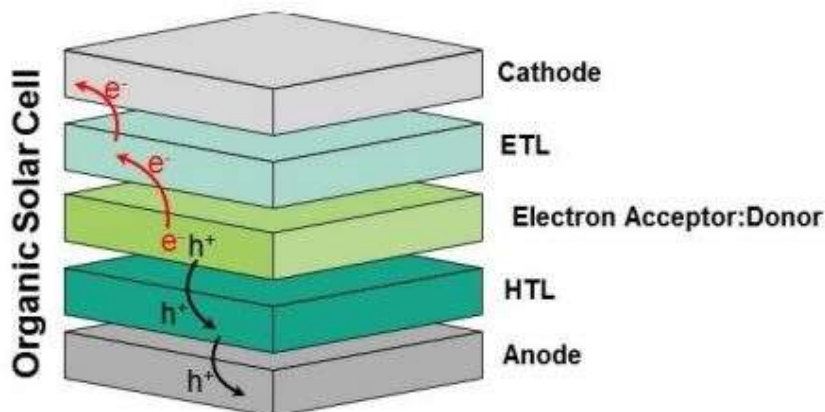


Figure 2.3: The structure of organic solar cell (Hashemi, Ramakrishna, & Aberle, 2020).

2.3 Recent development of flexible Solar PV

Although there are different research targeting on different type of solar cells, but most of the commercially available solar cells only include monocrystalline silicon cell, the amorphous silicon cell, and the polycrystalline silicon cell. However, most of the monocrystalline silicon cells and polycrystalline silicon cells are only slightly bendable compare to the other types of flexible solar PV, so they are ignored in this section. Flexible solar PVs that use solar cells such as OSC, PSC and DSSC are less common in the market and very expensive to purchase.

For example, companies such as Mekoprint and Solarmer focus on development and fabrication of organic solar cells for commercial use. However, due to the low efficiency with commercially available OSC materials, the market for OSC is still niche and hard to compete with other types of solar cells (Hösel, Angmo & Krebs, 2013). For PSC, due to low long-term stability and lack of suitable material and fabrication methods to develop high efficiency PSC in cheaper way, the commercially available PSC is still lacking (Zhang et al., 2017). DSSC, compare to other recent

technology, is already commercialize since 2009. But due to high material cost and low stability (Mozaffari, Nateghi & Zarandi, 2017), it is hard to purchase such Solar PV in the market.

For the amorphous silicon cell, there are many well-established companies that produce such cell, like Fuji Electric and HanHwa Q cells. This type of solar cell is often used in wearable technologies too. Although it still achieves low efficiency, but the lower cost of the cell makes it still investable for most of the consumers. Hence, this experiment is conducted using flexible Solar PV made of amorphous silicon cell.

2.4 Supercapacitor

With the flexible solar PV to harvest and generate energy, a storage medium will be required to store the energy and provide energy to the wearable technologies when there is no light to generate electricity. Hence, supercapacitors, also called electrochemical capacitor or ultracapacitors have fascinated industries due to its fast-charging rate and discharging rate, greater power burst, longer cycle life and high reliability compare to other energy storage such as fuel cells and batteries (Stoller, Park, Zhu, An & Ruoff, 2008). However, it has lower energy density compare to their size, high self-discharge rate, and voltage loss during discharge compare to batteries.

The main structure of a supercapacitor is composed of 2 electric conducting electrode, 1 electrolyte and 1 separator, where the active elements on electrodes are used to store ions and the conducting element of the electrode is used to pass the ions to the circuit as current, the electrolyte is used to store ions and the separator is to prevent mixing of ions in some of the EDLC to achieve better EDLC performance.

There are 3 main groups of supercapacitors in general with different charge storage mechanisms, which are the electrochemical double-layer capacitor (EDLC), the pseudocapacitor and the hybrid capacitor. The charge storage mechanism of EDLC is such that when electricity is provided to the EDLC, there will be charge separation occurs in the electrolyte, where positive charged ion will attract to the anode, while negative charged ion will attract to the cathode, then during discharge, attracted ions in the electrolyte will be released and current is produced as shown in Figure 2.4 (High Performance Electrical Double-Layer Capacitors DMF & DMT Series, 2020). EDLC is mainly dependant on the specific surface area of building materials, pore size and structures of the active elements and electrical conductivity of the materials. As no chemical reaction occurs during the charge-discharge mechanism of EDLC, it is

known to be able to repeatedly charge and discharge for a long time without losing performance, however the energy density of EDLC is lower than of the pseudocapacitor and hybrid capacitor.

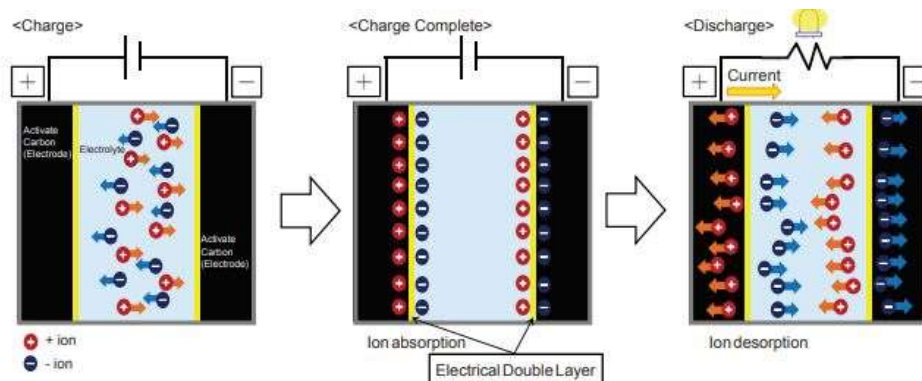


Figure 2.4: Illustration of charging and discharging mechanism of EDLC (High Performance Electrical Double-Layer Capacitors DMF & DMT Series, 2020).

Meanwhile, the charge storage mechanism of pseudocapacitor is different from EDLC, it mainly used chemical redox reaction on the surface of electron and reversible faradiac charge transfer process (Zhang, He, Shi & Zha, 2018). where during charging process, one of the electrodes will reduce the ion in electrolyte to anion and another electrode will reduce the ion to cation just like batteries. Then, the reaction is reversed during the discharging process as shown in Figure 2.5. However, in pseudocapacitor, the ions only adhere to the electrode and this allows fast redox reaction to occur and improve the speed of charge and discharge cycle. The geometrical configuration, electrical behavior and theoretical capacitance of the electrolytes and electrodes will affect the capacitance and properties of pseudocapacitor. For the hybrid capacitor, it is the combination of EDLC or pseudocapacitor at one side with lithium batteries at the other side. As both pseudocapacitor and hybrid capacitor have chemical reaction during charging process, they will have irreversible components during the charge-discharge cycle, the accumulation of the components will reduce efficiency of the capacitors over time. Hence, they both poses greater charge storage and capacitance while having lower durability.

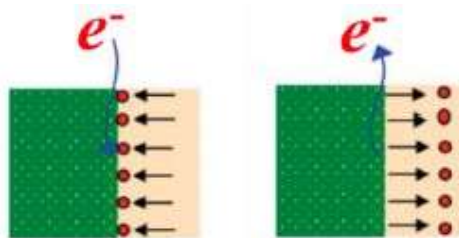


Figure 2.5: The illustration of charging-discharge mechanism of pseudocapacitor (Zhang, He, Shi & Zha, 2018).

2.5 Electrodes and Electrolyte used for the EDLC

The major problem with EDLC is that the energy storage is too low to replace battery as storage medium, as the energy density is often lower than commercially required. Hence, both electrode and electrolyte material of EDLC is required to be improved. In a study conducted by Wu & Cao, (2018), shows that energy density can be improved by increasing the capacitance and working voltage of the EDLCs, which is done by allowing electrode to have higher effective surface area, increasing the window voltage of the electrolyte and enhancing the volume, porosity, pore size and the ionic size of the material. For pore size of the electrodes and the ion size of electrolyte, normally, the smaller the pore size will often result in a higher surface-to-volume ratio of the electrode, which will increase the capacitance, However, one research from Largeot et al. (2008) shows that the electrode pore size and the electrolyte ion size must be at the same size to achieve maximum capacitance. Furthermore, another research from Heimböckel, Hoffmann & Fröba (2019) also proved that the although smaller pore sizes (lower than 1nm) can perform better than larger pore size, but the pore size with lower than 4nm can reduce the capacitance of the EDLCs as the accessible surface area for ion is lowered with the smaller pore size. To amplify the porosity and surface area of the electrode, one approach is using metal-organic frameworks (MOFs) at the electrode, which shows greater porosity and surface area rather than carbon-based material. However, MOFs generally have lower electrical conductivity, but in one study demonstrated by Sheberla et al. (2016) shows that a type of MOF, $\text{Ni}_3(2,3,6,7,10,11\text{-hexaiminotriphenylene})_2$ ($\text{Ni}_3(\text{HITP})_2$) has high electrical conductivity can create high capacitance with a high capacity retention rate too.

Other than electrode, the electrolyte of the EDLCs also play a big role in improving the energy density stored in supercapacitors. As the electrolyte used can

influence the working voltage of the EDLCs, which can affect its energy storage. Based on study from (Wu & Cao, 2018), electrolyte material can have great influence on the energy stored. By using the aqueous electrolyte system, which have less than 1 V of working electrolyte voltage, stores the least energy, compare to organic electrolyte with more than 2 V of working voltage and ionic liquid electrolytes (ILs) with more than 3 V of working voltage. However, ILs often associate with lower ionic conductivity and reduced capacitance. Hence, a recent approach mixed ILs with organic solvent to produce electrolyte with high working voltage and high capacitance. In one approach, as shown in a study, the addition of γ -butyrolactone (GBL) in EMIMBF₄, a binary electrolyte is formed and is able to hit 3.7V of working voltage (Tian et al., 2018). Furthermore, some approaches focus on mixing of organic solvent with inorganic material to create high working voltage electrolyte. An approach in another study shown that mixing of NaPF₆ salt in 1,2-dimethoxyethane (DME), which is a type of organic solvent can improve the working voltage to bigger than 3.5 V (Ruther et al's, 2016). However, the electrolyte must be able to cope with electrode material to produce highest energy storage.

Although liquid electrolyte can often show great ionic transportation and make great EDLCs, but the liquid state electrolyte is undesirable for flexible application as liquid electrolyte cannot be contained easily. Hence, another approach used solid state electrolyte to construct EDLC, but when the electrolyte is in solid state, it is not flexible. So, gel state electrolyte is useful when building ready to use EDLC, as gel state electrolyte has higher ionic transportation rate and flexibility compare with solid state electrolyte, does not have electrolyte leakage problem and has smaller solvation shell as compare to liquid state electrolyte (Pullanchiyodan et al., 2020). Hence it is desirable to be electrolyte of EDLC. One of the material for solid state electrolyte is PVA, which can be used to construct gel state electrolyte, several studies shows the EDLC that uses PVA based polymer shows better cycle life and greater capacitance compare to liquid state electrolyte with separator (Yang, Hsu & Chien, 2005).

2.6 Architecture of flexible EDLC

With the increasing interest in fully flexible wearable technologies, integration of flexible EDLCs with flexible solar PV have attracted more interests. Unlike EDLCs, flexible EDLCs requires all of its components to be bendable, scalable, non-toxic, non-flammable, light in weight to meet the needs (Li, Wu, Yuan & Zhang, 2014). The

structure of flexible EDLCs is the same as EDLCs, which consist of active electrodes, current collectors, electrolyte and separator. There are several types of architecture of flexible supercapacitor which are fiber-like flexible supercapacitors, paper-like flexible supercapacitor and 3D porous flexible supercapacitor currently being developed (Dong et al., 2016).

For fiber-like flexible EDLC, there are 2 types of structures, which for the first type, the structure is twisted together to form a helical shape and the another type is the material wrapped around each other to form a coaxial structure as shown in Figure 2.6.

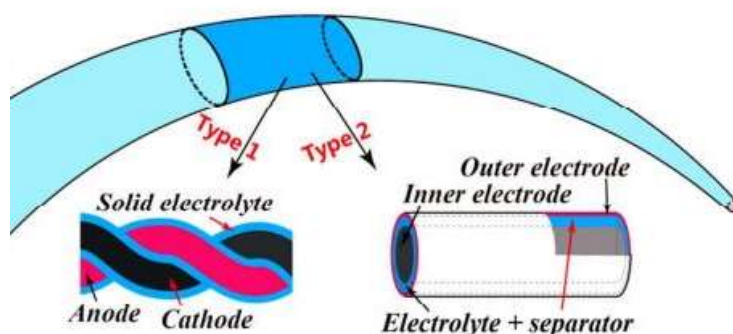


Figure 2.6: Figure of various type of build for fiber-like flexible supercapacitor (Dong et al., 2016)

One of the construction is where the plastic fibre is used to construct the EDLC, the plastic fibre is coat with commercial pen ink and used as electrode, then the electrode is weaved in helical shape separated by spacer wire. This construction can achieve maximum of 19.5 mF cm^{-2} , energy density of maximum $2.7 \times 10^{-6} \text{ Wh cm}^{-2}$ and no degradation after 15000 cycles (Fu et al., 2012). However, with the insulation of plastic fibre, deposition of conductive film on the fibre is often needed, which will increase the complexity and cost of fabrication of the fibre. Another approach is the direct use of metal fibre in the EDLC, with electrical conductivity and bendable properties in metal material, it will be easier to fabricate such materials than plastic. A researcher has conducted a study to use copper fibre as the base, coated with Chinese ink with carbon and binder as electrode materials to produce metal fibre EDLC that has specific capacitance of 34.5 mFcm^{-1} (Zhang et al., 2015). However, metal fibre is heavy and unsuitable for wearable technologies, so the carbon fibre,

which is light in weight and have electricity conductivity is used for EDLC. In one study, carbon fibre is cured with organic acid and heated to 950°C under nitrogen to produce carbon fleece and perform similar to than platinum based EDLC (Josef, Yan, Guterman & Oschatz, 2019). However, the high price tag come with carbon fibre is still a problem faced by carbon fiber cloth. So, textile or yarn which is small in diameter, cheaper than carbon fibre, lighter than metal, and more environmental friendly than plastic fibre is used to produce electrodes of EDLC. However, one disadvantage of using textile or yarn in construction of EDLC is that these materials are electric insulator and required extra fabrication to conduct electricity. Furthermore, they will need to use add carbon coating on top of the textile to become EDLC. However, there is one approach which use knitting machines to embed cellulose based yarns with different kind of carbons based material on it and produce supercapacitors (Jost et al., 2014).

For paper-like flexible EDLC, which is also called planar flexible supercapacitor, is different in architecture than fibre structure. Rather than using long string of fibres, the electrodes, electrolyte and separator are stacked together in thin sheets along with packing shell and current collector as demonstrated in Figure 2.7.

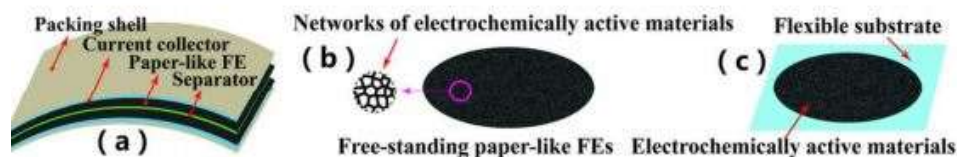


Figure 2.7: Figure of paper-like FSCs is shown in part (a) of the figure, free-standing paper-like FEs is shown in part (b) of the figure and the flexible substrate supported FEs is shown in part (c) of the figure (Dong et al., 2016).

The planar flexible supercapacitor can be grouped into 2 classes, which are free-standing flexible EDLC and substrate supported flexible EDLC. For free-standing flexible EDLC, the electrode of the EDLC often have strong structure that can support itself , the structure is often associated with pores to allow interaction between electrolyte and electrode. No external supports/ substrates are needed to hold the structure in shape. While substrate supported paper-like flexible EDLC will have substrate to support their structure, the electrode of these structure is normally

constructed from metal hydroxide or metal oxide, as they, unlike carbon-based materials, are fragile in properties and hard to build free-standing structure (Dong et al., 2016). Planar flexible supercapacitor structure when use with solid-state electrolyte, can build full solidstate supercapacitors. Carbon nanotubes (CNTs) which can be single-wall or multi-wall is used to build free standing planar flexible EDLC. One approach is to coat single-walled CNTs onto cotton paper to make the electrode and use solidstate polymer for the electrolyte to build supercapacitor. Such full solidstate flexible supercapacitor can have maximum 48.8587 Wh/kg energy density and 115.8301 F/g specific capacitance (Hu, Rajamani & Yu, 2012). Furthermore, CNTs also can be used with supporting substate to build high capacitance EDLC. One approach is by coating Polyaniline (PANI), which is a flexible and conducting polymer onto CNTs to enhance the flexibility and specific surface area of the electrode. When the electrode is paired with H₂SO₄-polyvinyl alcohol gel as electrolyte, a simple yet high capacitance (31.4 F/g) EDLC is built (Meng, Liu, Chen, Hu & Fan, 2010) as shown in Figure 2.8.

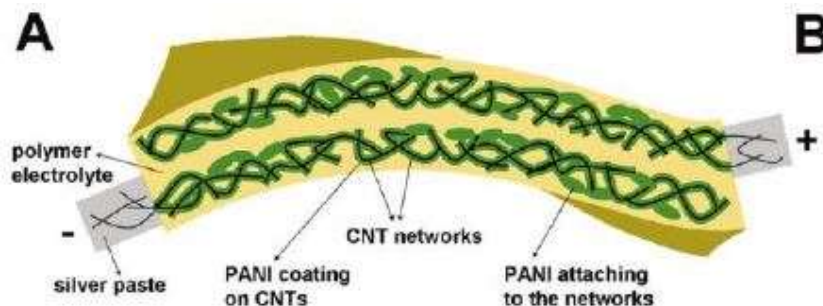


Figure 2.8: Structure of PANI coated CNTs electrode. (Meng, Liu, Chen, Hu & Fan, 2010).

Other than CNTs, there is another approach to build paper-like supercapacitor. Carbon based material such as carbon fibre papers can be used to grow other structure on it to build better paper-like electrode. Such add on on carbon structure will allow significantly higher amounts of electroactive pores on the surface and allow higher amount of electrolyte to passthrough, which result in better capacitance. For example, one research has showed that by vertically growing MnO₂ nanorods on the substrate have improve the capacitance of the material, while maintening the flexibility of the material as shown in Figure 2.9 (Dubal, Kim, Kim, Holze & Kim, 2013). Hence, the

similar technique can be used to improve the performance of carbon-based substrate. Another study conducted that uses conductive carbon fiber to grow MnO_2 nanosheet array, when this material is paired with graphene that grow on carbon fiber, a flexible supercapacitor with high specific capacitance, 87.1Fg^{-1} with 95.2 % capacitance retention after 3000 cycles is developed, which shows great stability in the supercapacitor (Yu et al., 2015). The similar technique can also be used to grow carbon-based material on metal substrate to achieve higher conductivity and and specific surface area electrodes. Another research has used the similar technique in growing CNTs on Fe-Ni based metal alloy foils to make electrodes and successfully obtain relatively good specific capacitance flexible EDLC (Seman, Azam & Mohamed, 2016). Furthermore, there is also another technique that use thin-film technique to produce thin film carbon-based electrode, which the thickness of the carbon film is extending from nanometres to micrometres. This type of electrode can construct better EDLC with higher flexibility and faster electrochemical response (Yu & Feng, 2019).

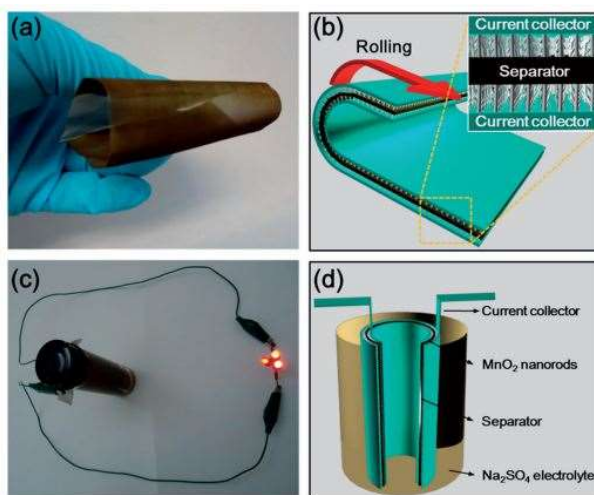


Figure 2.9: (a) Figure shows bending of flexible MnO_2 electrode which consists of large surface area (b) Figure shows structure of the EDLC which consists of one separator and MnO_2 electrodes. (c) Set-up used for the actual demonstration of the flexible MnO_2 electrodes. (d) The structure of flexible MnO_2 supercapacitor (Dubal, Kim, Kim, Holze & Kim, 2013).

Another architecture of flexible EDLC is 3D porous flexible EDLC. Unlike fibre-like and paper-like supercapacitor, which store limited amount of energy due to thin in thickness as increase in thickness will reduce capacitance capability of the

supercapacitor (Hu et al., 2009). The 3D porous flexible EDLC use similar approach as paper-like supercapacitor, but instead of a thin sheet, it uses 3D porous structure as electrodes, where a 3D flexible porous structure with greater thickness and higher surface area is used as electrode. The porous structure will allow better flexibility of the material, allow greater ion movement inside the material, and able to store greater amount of electrolyte which leads to higher energy stored inside the EDLC. One of the 3D porous flexible electrodes for EDLC is textile, which including polyester microfibre, cotton cloth and carbon fibre fabric (Jost, Dion & Gogotsi, 2014). The textile electrodes must have several properties to serve as electrodes, which are great electrochemical properties, flexible and great electricity conductivity. Some of the textile that doesn't poses such properties can also be modified by coating on the textile, this modification can hold the properties of the textile, such as thickness and porous structure while having the properties of the coating too. One research study shows that the by using "dipping and drying" method with single walled carbon nanotube (SWCNT) ink on textile, which is a cotton fibre, have introduced coating on the textile structure. This makes the coated cotton textile to have flexibility, electrical conductivity, higher porosity, higher thickness for the electrolyte to react and higher areal capacitance of the textile. These modified textiles have electrical resistance of $4 \Omega/\text{sq}$ and can construct EDLC supercapacitor with capacitance up to 0.48Fcm^{-2} with high specific energy as shown in Figure 2.10.

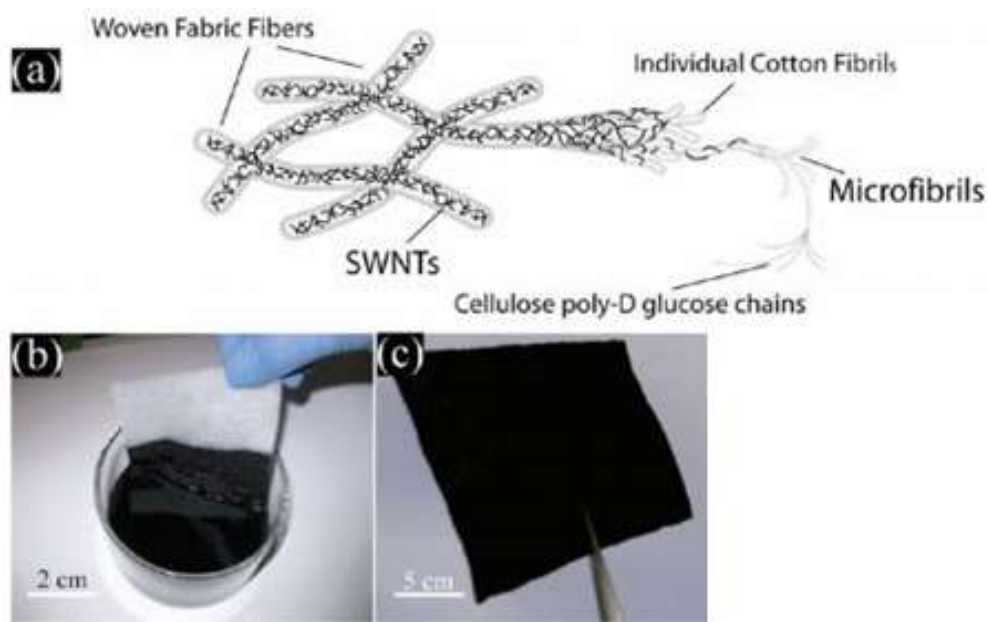


Figure 2.10: (a) Figure shows cellulose fibers is wrapped by SWNTs to form the individual cotton fibrils, and stacked fibrils to form 3D porous structure. (b), (c) By dipping textiles into an aqueous SWNT ink and dried by oven under 120 °C for 10 mins to make conductive fibre (Hu et al's, 2010).

Although the coating of carbon nanotubes on the cotton will make cotton an electrode with good electrical conductivity, however, the conductivity is less and possesses high electrical resistance when compared to metal, which can greatly reduce the ionic transport and insertion of ions into the active material structure that can store ions, and reduce the total capacitance of the supercapacitor (Moazami, 2017). There is one study which adds a metal collector layer to the carbon-based electrode, which raises the specific capacitance of the supercapacitor to about 60 folds of the supercapacitor without a metal layer, with higher conductivity metal layer, copper shows higher specific capacitance compared to gold shows better specific capacitance of the material (Li, Mak, Kan & Hui, 2014). Hence, it can be predicted that by coating a silver layer, which is the highest conductivity material, onto the fabric can greatly increase the specific capacitance of the carbon-coated fabric.

Instead of textile, there is also another approach that uses graphene foam, which has properties of flexibility, high thickness, and 3D porous structure as an electrode. Then, electricity-conducting materials are bound to the structure and act as an electrode. In one study conducted, which bonded highly conductive graphene sheets with Ag-conductive

epoxy to form a graphene-Ag-3D graphene foam as shown in Figure 2.11. This material is used to build electrode and shows high areal capacitance of 38mFcm^{-2} at 0.67mAcm^{-2} (Manjakkal, Núñez, Dang & Dahiya, 2018).

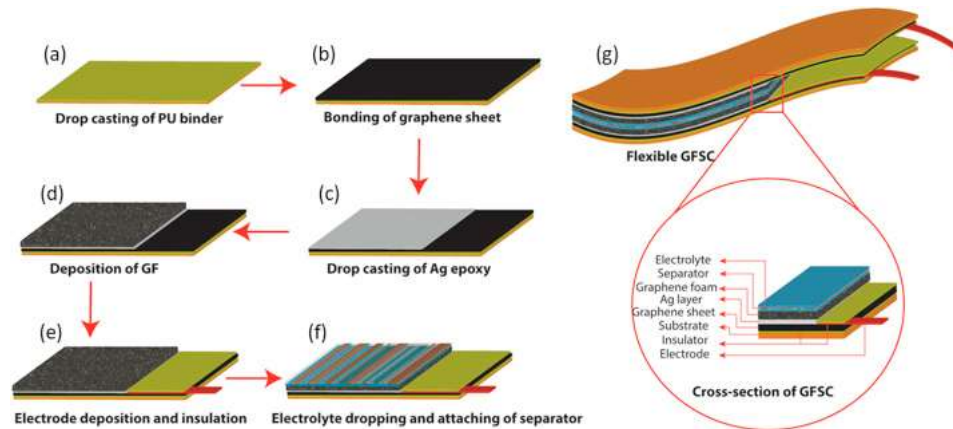


Figure 2.11: Steps to fabricate GFSC electrodes to assemble into complete GFSC fill cell (Manjakkal, Núñez, Dang & Dahiya, 2018).

2.7 Performance measurement of the hybrid device

For flexible solar cells, there are several parameters is required to be measured to understand the performance of the solar cell. First, the energy conversion efficiency of solar cells, η can be calculated by Equation 2.1.

$$\eta = \frac{P_{max}}{E_{tot}A} \quad (2.1)$$

Where

η = Efficiency of solar cells

P_{max} = Solar PV maximum power output, W

A = Surface area of the solar PV, m^2

E_{tot} = Total irradiance that the solar PV is exposed, Wm^{-2}

However, total irradiance of the solar PV is highly dependence on the intensity, spectrum and illumination density of the light the solar PV is exposed to, and it is hard to be fixed for measurement. Hence, total irradiance of 1000Wm^{-2} is used to represent full sunlight condition, under 25°C ambient condition. In order to generate approximate total irradiance, a full spectrum light source is used to simulate sunlight, and optical homogenizer is used to spread the light intensity evenly on the surface of

the solar PV, which an apparatus called solar simulator is often used to produce suitable sunlight (Field, 2017). To measure the maximum power output, IV-curve will be plotted, where the short circuit current and open circuit voltage are measured to calculate the power output of the solar PV.

Furthermore, to measure the performance of the capacitance of EDLC, cyclic voltammetry test can be used to measure the areal capacitance, voltage windows and cycle life of the EDLC (Cyclic Voltammetry, EIS, Leakage Current-Testing Electrochemical Capacitors, 2020). After that, we can calculate the energy density and power density of the system.

Then, the performance of the flexible solar PV and EDLC system is measured based on overall efficiency of energy conversion. It measures the proportion of output energy that is generated by the whole system with the total input energy, which is the light energy that is input into the system.

The overall efficiency of most of the solar PV, supercapacitor and battery system will be around 5% while some of the research shows efficiency as high as 8.1% (Yuan et al., 2019).

2.8 Recent development of the hybrid device

The combination of flexible solar PV with flexible EDLC can produce a self-charging energy storage system that can be integrated into different technologies. There are several approaches demonstrated by different study regarding this, however, most of the approaches still face great amounts of challenges like mechanical instability of the structure, low energy efficiency, safety issues, effect of miniaturization on the system, comfort to the user and sustainability of the device (Tang et al., 2020). For example, a study has demonstrated the polypyrrole-based supercapacitor that store energy and uses silicon nanowire heterojunction solar cell to harvest solar energy simultaneously can have 10.5% total conversion efficiency (Liu et al., 2017). Furthermore, another system developed has demonstrated another approach in the fully hybrid integrated system, where both the solar cells, sensors, and energy storage are printed on a flexible substrate, which forms a planar like fully integration structure (Lin et al., 2018). However, the system only delivers 12.9 mFcm^{-2} of capacitance, so the energy that can be stored is still less expected.

2.9 Summary

More efforts are needed to pair up EDLC with solar cells to convert a higher amount of sunlight into electricity and the EDLCs require greater modification to store enough energy so that such wearable technologies can be commercialized.

One approach that can speed up the time to commercialize hybrid EDLC with flexible solar PV is by building flexible solar PV with EDLC from commercially available materials. Hence, flexible solar PV that are purchased from the market can be connected to EDLC which electrode made of commercially available metal coated textile. As both are highly flexible materials, so these 2 materials can be knit together to become smart clothing easily. Furthermore, several modifications on the EDLC and flexible solar PV is required to ensure the end product can be commercialized.

CHAPTER 3

METHODOLOGY AND WORK PLAN

3.1 Introduction

The research will be based on hybrid flexible solar PV with flexible textile based EDLC. The flexible amorphous silicon thin-film solar PV is outsourced from WarmSpace Technology. Then, the flexible textile based EDLC is made from commercially available silver coated textile, which is fabricated by adding activated carbon coating in the lab. After that, the system is assembled together, where efficiencies, input and output of the integrated system is recorded.

3.2 Methodology

To investigate the capabilities of hybrid flexible solar PV with flexible fabric based EDLC, the materials and methods used to build the silver fabric based EDLC is introduced. Then, the capabilities of the EDLC is investigated using different testing method. After that, the performance of the EDLC when connected with the flexible solar PV is investigated experimentally to ensure the viability of such design in real life.

3.2.1 Flexible solar PV

As it is used in the wearable technology, the flexible solar PV should have enough efficiency to convert sunlight to electricity at outdoor, water-resistance, flexible, light, durable, can be sew together with textile, commercially available and cheap. The most suitable material will be amorphous silicon based solar cell. Based on the criteria, we need to achieve higher light absorption and efficiency of the solar cell, so multilayer thin film structure is used, where greater spectrum of light can be converted to electricity. Furthermore, with multilayer film structure, the silver and zinc oxide substrate at the bottom of the sheet will be used to reflect the unabsorbed light from the solar cell back to the top to be re-absorbed again, resulting in higher efficiency. Furthermore, to achieve the water resistance, durable structure and sew, the multilayer film is covered under ethylene tetrafluoroethylene (ETFE). This flexible solar PV is obtained from WarmSpace and is shown in Figure 3.1, where according to the specifications listed, the efficiency of the flexible solar PV can reach maximum of

10%. The flexible solar PV has working voltage of 6 V, working current of 0 – 330 mA, open circuit voltage of 7.2 V and short circuit current of 350 mA. The output power is 2 W under light intensity of 1000 W/m² and light spectrum AM 1.5.



Figure 3.1: Photo of flexible solar PV from WarmSpace, which use multiple layers of amorphous silicon solar cell and packed with ETFE technology.

3.2.2 Flexible fabric based EDLC

The flexible fabric based EDLC is based on the study, where the commercially available metal coated conductive fabric coated with activated carbon paste is used as the electrodes and a solid-state gel electrolyte is used as electrolyte (Pullanchiyodan, Manjakkal, Dervin, Shakthivel & Dahiya, 2020).

To fabricate the electrodes of the EDLC, commercially available silver coated conductive fabric from brand Green Phil, which is under dahuakangqiao.ltd from China is cut into multiple small pieces with area of around 25cm² each and weighted to get an average weight the pieces. Then, carbon paste is prepared with 1.8 g of activated carbon powder, 0.2 g of PVDF, and 30 mL of Acetone mixed under continuous stirring at room temperature for 2 hours under 50°C and 600 rpm as shown in Figure 3.2. After that, the carbon paste is applied to one side of the silver coated conductive fabric surface using a brush. Then, the fabric is dried in vacuum oven under 60 °C for 2 hours. The final product is used as the electrode of the EDLC.



Figure 3.2: Picture illustrates mixing of activated carbon coating (right) and PVA gel (left).

A 0.2mm thickness of aluminium sheet is cut into size of 25cm^2 , applied with carbon paste too using the similar method to prepare for the silver coated fabric for comparison study. The finished electrode is as shown in Figure 3.3.

After that, to ensure better average coating, another layer of activated carbon coating is applied onto the coated side of the electrodes for both, so most of the surface is covered with activated carbon. Then, the electrodes are weighted again to obtain the average weight of the active element, activated carbon, on the surface of the electrodes.



Figure 3.3: Photo of activated carbon coating applied on silver coated clothing (2nd row) and aluminium sheet (1st row) for the 1st time.

To fabricate the electrolyte of the EDLC, 10mL of water is used to dissolve 1g of Polyvinyl alcohol (PVA) under continuous stirring at 55°C for 4 hours until all the PVA is fully dissolved into the water. After that, 4.7g of 85% concentration H_3PO_4 solution is added into the mixture to achieve mass fraction of 0.79 with respect to PVA. Then, the mixture is mixed for another 1 hour with continuous stirring at 50°C at 800 rpm as shown in Figure 3.2. After that, the final solution is poured into the petri dish and covered with aluminium foil as shown in Figure 3.4. Then, the gel electrolyte is dried under 60°C for 4 hours and dried at the room temperature for another 1 day before use.



Figure 3.4: Liquid form of H_3PO_4 gel electrolyte after 5 hours of mixing.

After that, the electrodes and the electrolyte are assembled into EDLC. First, half of the carbon coated side of the silver coated fabric is put on the petri dish that contains the electrolyte. The gel-based electrolyte is sticky and can easily stick to the electrode when the electrode is removed. Then, another layer of carbon coated side of the silver coated fabric is used to sandwich the electrolyte. To ensure stability of the EDLC, a 5 kg object is used to press the EDLC for 10 minutes. The carbon coated 0.2 mm aluminium sheet EDLC is also prepared under similar method. The final product of the EDLC is shown in Figure 3.5.



Figure 3.5: Figure illustrates fabricated EDLCs made of silver cloth (left) and aluminium sheet (right).

3.3 Characterisations

There are several data to be collected in this project. First, the flexible solar PV will be placed at low light location and strong light location. Then, the open circuit voltage, V_{oc} and short circuit current, I_{sc} will be measured using a multimeter, where the positive anode and negative cathode of the flexible solar PV is connected to the positive terminal and the negative terminal accordingly as shown in figure 3.6. Then, using V_{oc} and I_{sc} that are recorded, we can obtain the actual power output of the solar PV under the condition that we set to predict the performance of the solar PV and its interaction with EDLC. This test is to test for the power output of the solar PV under different light source to check if solar PV can generate enough electricity to power up electronics in low light condition, where the irradiance is 100 W/m^2 and high light condition, where the irradiance is 1000 W/m^2 .



Figure 3.6: Measurement on flexible solar PV using multimeter.

For the flexible EDLC, the conductivity and working voltage of the electrolyte material is measured using conductivity test and linear sweep voltammetry test with a potentiostat as shown in Figure 3.7. The specific capacitance, areal capacitance, power density and energy density of the flexible EDLC is measured with electrochemical impedance spectroscopy test (EIS). Furthermore, the stability of the EDLC is measured using Galvanostatic charge/discharge (GCD) analysis using constant current / constant voltage test (cc/cv test). To make comparison to the silver cloth based EDLC, an aluminium sheet is used to build the EDLC with similar method, and the comparison between the two types of EDLC is shown.



Figure 3.7: Figure shows EIS conducted on PVA gel electrolyte measured with ZIVELAB potentiostat.

Last but not the least, the assembly of the hybrid flexible solar panel with flexible EDLC will be carried out. The solar PV is connected to the EDLC and connected to the LED, where the LED is acted as a load.

To test the hybrid, it will be first exposed to strong light for 10 seconds. Then, the solar PV will be disconnected from the flexible EDLC, while EDLC is connected to a multimeter to measure the voltage output, the time for the EDLC to release voltage between 1.8V to 3.3V is recorded using a multimeter. The voltage set to be 1.8V to 3.3V because red LED have a forward voltage of minimum operating voltage of 1.8V and maximum operating voltage of 3.3V. When voltage higher than 3.3V is applied, where the solar PV supplied 7V, the LED is burn and the experiment result is not usable. The method to measure the result is shown in Figure 3.8 and Figure 3.9, and the circuit connection of the circuit during EDLC charging and EDLC discharging is shown in Figure 3.10.



Figure 3.8: Photo shows the method used to charge EDLCs with solar PV, where the multimeter is parallel to the circuit of solar PV and EDLC to measure the voltage provided by the solar PV to EDLC.



Figure 3.9: Photo shows the method used to measure the discharge EDLCs using multimeter.

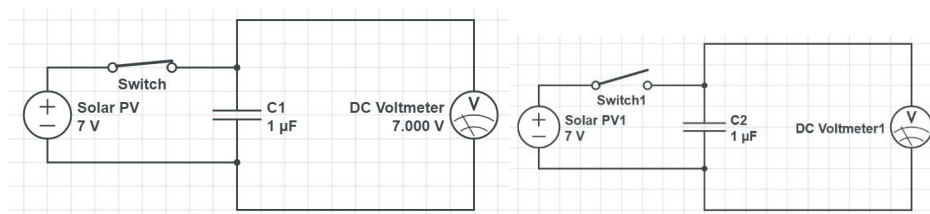


Figure 3.10: Photo shows the circuit diagram used to measure the performance of EDLC and Solar PV, where C1 and C2 is the silver coated textile EDLC, and the DC Voltmeter is the multimeter, voltage source is the solar PV. The left shows the circuit diagram during charging of the EDLC and the right shows the circuit diagram during discharging of the EDLC.

3.4 Work Plan

The work plan of this project is shown in Table 3.1 and Table 3.2, where the schedule is planned carefully to build and test the hybrid within the time limit.

Table 3.1: Gantt chart of the experiment works

Activities			Duration (Days)
Start Date	End Date	Description	
14/9/2020	15/11/2020	Purchase of silver coated fabric, graphite powder, silver wire, silver epoxy, LED strip, wearable temperature sensor and flexible solar PV	45
15/11/2020	1/11/2020	Measurement of flexible solar PV outputs	17
1/11/2020	10/11/2020	Making of fabric based EDLC	10
10/11/2020	1/12/2020	Measurement of flexible fabric based EDLC	20
1/12/2020	2/12/2020	Assembly of hybrid flexible solar PV with flexible EDLC	1
2/12/2020	5/12/2020	Measurement of hybrid flexible solar PV with flexible EDLC	3
5/12/2020	10/5/2020	Assembly of sensors and LED strips to the hybrid flexible solar PV with flexible EDLC	5
10/12/2020	26/12/2020	Final testing for functionalities of prototype	10
26/12/2020	6/3/2020	Data Analysis	11
6/3/2020	17/4/2020	Documentation and final report preparation	30

3.6 Summary

Hence, the experiment is well planned to perform analysis of the hybrid flexible solar PV with EDLC made with commercially available silver coated fabric-coated with activated carbon paste as electrode. The prototype of such hybrid will be made with the performance measured and result recorded to find out if such hybrid is functional in practical application.

CHAPTER 4

RESULTS AND DISCUSSION

4.1 Conductivity of gel electrolyte

The gel electrolyte is first tested for conductivity. This is because solid electrolyte generally has lower conductivity than the electrolyte in liquid form due to lower ionic mobility. As electrolyte conductivity can influence EDLC's capacitance and operating voltage, good electrolyte conductivity is required for higher capacitance EDLC.

To calculate conductivity of the electrolyte, we will need bulk resistance, area of the measured electrolyte and the thickness of gel electrolyte. The bulk resistance of the electrolyte is obtained using potentiostat. With EIS, nyquist plot of the electrolyte is obtained. The settings of the potentiostat EIS is stated in Figure 4.1, where the initial frequency is 1×10^6 Hz and the final frequency is 1×10^{-3} Hz. By plotting it on a graph it will show a semi-circle shape. Using ZMAN software, the diameter of the semi-circle shape is computed as shown in Figure 4.2.

ITEM	VALUE	Option
Initial delay	<input checked="" type="checkbox"/> Enable	
-Duration(s)	1:40	
-Stability(V/s)	1000.0e-9	
Bias potential(V)	0.0000e+0	ERef <input type="button" value="v"/>
Amplitude(V)	10.000e-3	
Initial freq.(Hz)	1.0000e+6	
Middle freq.(Hz)	1.0000e+6	
Final freq.(Hz)	100.00e-3	
Sweep type	Log <input type="button" value="v"/>	
Density	10	
Iteration	1	
Init. I Range(A)	1 A <input type="button" value="v"/>	<input checked="" type="checkbox"/> Auto
Speed	Normal <input type="button" value="v"/>	

Figure 4.1: Potentiostatic EIS static set-up setting to measure the conductivity of the electrolyte.

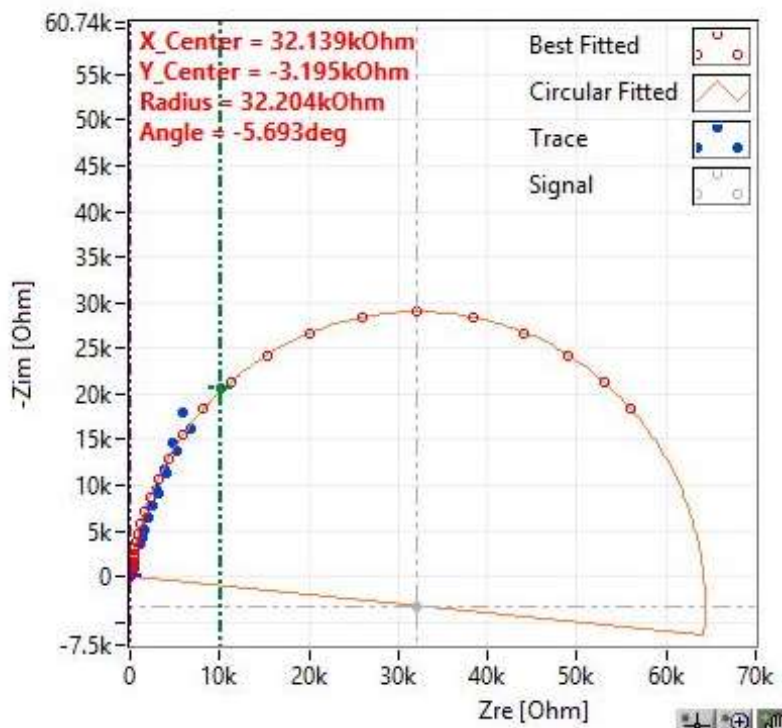


Figure 4.2: Nyquist plot of the electrolyte, plot with Potentiostat EIS shows the bulk resistance of sample 1 is 64.278 k Ω .

By using graphical analysis on the Nyquist plot, where the diameter of the circle at positive value of the circle is plotted, we can obtain the bulk resistance of the electrolyte. The thickness of the electrolyte is measured to be 0.0005 m using a micrometre, with 3 samples show different thickness when measured. Then, the area of the electrolyte measurement is same as the detectable area of the holder, which is 0.00031416 m².

By using all the values, ionic conductivity, σ of the gel-based electrolyte is obtained by Equation 4.1.

$$\sigma = \frac{t}{A \times R_b} \quad (4.1)$$

where

σ = ionic conductivity

t = thickness of the electrolyte, s

A = area of the electrolyte measured, m^2

R_b = bulk resistance of the electrolyte, Ω

The calculation is repeated for 2 trials to get a more accurate ionic conductivity of the electrolyte as shown in Table 4.1. Hence, based on the measurement, the ionic conductivity of the electrolyte is $0.00002954 \text{ Sm}^{-2}$. The measured result of the electrolyte is poor in conductivity, when compare to previous study where ionic conductivity of 820 Sm^{-2} (Alipoori, Mazinani, Aboutalebi & Sharif, 2020). The poor conductivity is due to the instrumentation error, lack of doped material in the PVA gel electrolyte, where the movement ionic conductivity is restricted and also the oxidation of PVA gel electrolyte, as the gel electrolyte is measured 1 week after it is made.

Table 4.1: Measurement of conductivity of different samples.

Sample	Thickness, t (m)	Area, A (m^2)	Bulk Resistance, R_b (Ohm)	Ionic Conductivity, σ (S/m)
1	0.0005	0.00031416	64278	0.00002476
2	0.0002	0.00031416	22504	0.00002829
3	0.0001	0.00031416	8950	0.00003557
Average				0.00002954

The conductivity of the electrolyte is also not as good as actual H_3PO_4 , which is relatively low compare to liquid state electrolyte. This may due to solid state gel highly restricts the ability of the ion inside the gel to move, and cause such low conductivity. However, such conductivity is still usable in constructing workable electrolyte.

However, there might be some error during the analysis and the measured value might defer from the actual value. First, the graph plotted in this experiment is not a complete semi-circle, this is mainly caused by the instrumental error and human error

when conducting the experiment. The holder used to hold the electrolyte together is not in perfect shape, when closing the lock of the holder, the lock will always be slanted by 10 to 20 degrees. This will cause the lock to be unable to press all the area of the electrolyte completely. The gaps caused by instrumental error will cause the result to have error. The electrolyte is also not in complete solid form but gel form. Hence, when closing the holder, the lid is required to be spun to close it, during the spinning, the gel may follow the lid to spin and cause error in measurement.

The thickness of the electrolyte is hard to measure accurately. As the electrolyte is in gel form but not in complete solid form, Hence, during measurement, when force is exerted to the electrolyte, the thickness of the electrolyte measured will change. Furthermore, when closing the lid, the electrolyte will be pressed too and change the electrolyte's actual thickness. Hence, the actual measured thickness is easily affected and maybe thinner than the measured value.

4.2 Potential windows of the electrolyte

Before constructing the EDLC, Linear Sweep Voltammetry (LSV) is conducted to measure the voltage stability of the electrolyte. The setting of the LSV as shown in Figure 4.3, where a scan rate of $20 \times 10^{-3} \text{ Vs}^{-1}$ is used and the potential measured is from -3 V to 3 V, the electrolyte is measured under room temperature. By comparing 5 trials of the electrolyte samples, we can obtain that the PVA gel-based electrolyte has a potential windows of 3Vs, which is from -1.5 V to +1.5 V as shown in Figure 4.4. Based on the result, the working voltage of our PVA electrolyte is 1.5 V when positively charged or negatively charged. The electrolyte is lower compare to previous research where 2.1 V is achieved, this may due to wrong composition of the electrolyte used in this experiment, where there is no doped materials (Brza et al., 2020).

* Technique - Linear sweep voltammetry

Parameters | Information

ITEM	VALUE	Option
Initial delay	<input checked="" type="checkbox"/> Enable	
-Duration(s)	1:40	
-Stability(V/s)	1.0000e-3	
Deposition	<input type="checkbox"/> Enable	
-Potential(V)	3.0000e+0	ERef ▼
-Duration(s)	0	
Quiet time(s)	2	
Initial potential(V)	-3.0000e+0	ERef ▼
Final potential(V)	3.0000e+0	ERef ▼
Scan rate(V/s)	20.000e-3	
Sample interval(V)	1.0000e-3	
IR Comp.	None ▼	
PF IR(ohm)	0.0000e+0	
I Range(A)	1 A ▼	<input checked="" type="checkbox"/> Auto

Figure 4.3: Settings of Linear Sweep Voltammetry analysis.

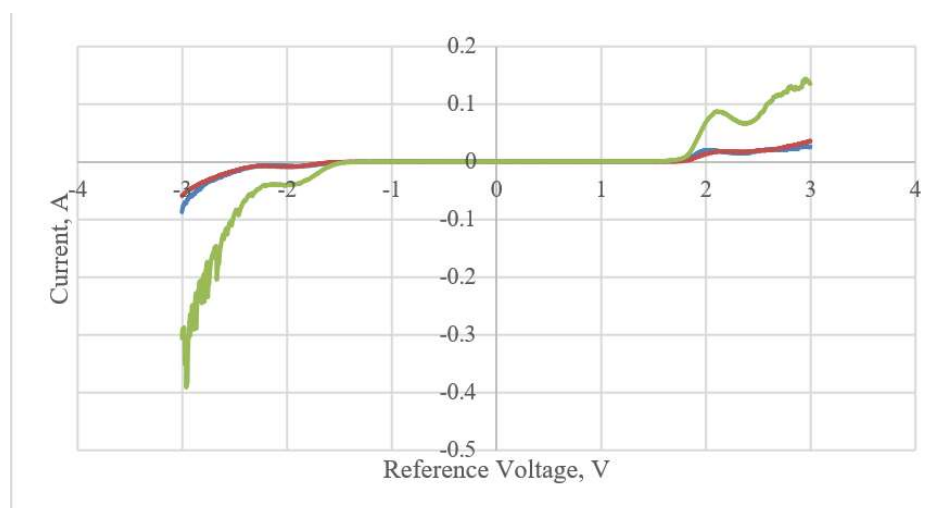


Figure 4.4: Linear Sweep Voltammetry of the electrolyte. Where the graph is flat from -1.5V to 1.5V, which represents the potential windows of the electrolyte.

4.3 Physical Properties of the EDLC

The 25 cm² silver cloth based solid state EDLC weighted 0.92 g and have high flexibility. It can be stretched for 10 % of its original length and able to return to its original shape. It can also bend to 90 degrees and roll into different shapes without any problem as shown in Figure 4.5. The high flexibility and lightweight shows great use in wearable technologies. As the EDLC is made of cloth, it is able to sew onto different cloths and plastics easily. Furthermore, the EDLC can be hold with bare hands without any problem, so solid-state EDLC is nontoxic and able to be handled easily.



Figure 4.5: Silver coated textile EDLC is rolled into round shape (Left 1) and bent 90 degrees (Left 2), the shapes of the EDLC still retains without any damage (Left 3).

4.4 Cyclic Voltammetry (CV) of EDLCs

In this experiment, areal capacitance and specific capacitance of the EDLCs are obtained. The areal capacitance of the EDLC is obtained by using Equation 4.2 and the specific capacitance of the EDLC is obtained by using Equation 4.3.

$$C_A = \frac{1}{2A\Delta V\nu} \int I dV \quad (4.2)$$

Where

C_A = Specific capacitance of the EDLC, F

$\int I dV$ = Area under the CV graph obtained, A

A = Active area of the EDLC, where electrolyte is sandwiched between the 2 electrodes, cm^2

ΔV = Electrochemical potential windows of the electrolyte, V

ν = Scanning rate used to get the CV curve, mV s^{-1}

$$C_p = \frac{\int Idv}{2m\Delta V\nu} \quad (4.3)$$

Where

C_p = Specific capacitance

$\int I dV$ = Area under the CV graph obtained, A

m = Mass of the active element, kg

ΔV = Electrochemical potential windows of the electrolyte, V

ν = Scanning rate used to get the CV curve, mVs^{-1}

The test is conducted on silver coated textile EDLC and aluminium sheet EDLC which is shown in Figure 4.6. The setting used for this CV analysis is as shown in Figure 4.7. The graph clearly shows that the silver cloth EDLC establish far greater area compare to aluminium sheet EDLC. The area under the curve is calculated using OriginPro software by integrating the area covered by the graph as shown in Figure 4.8.

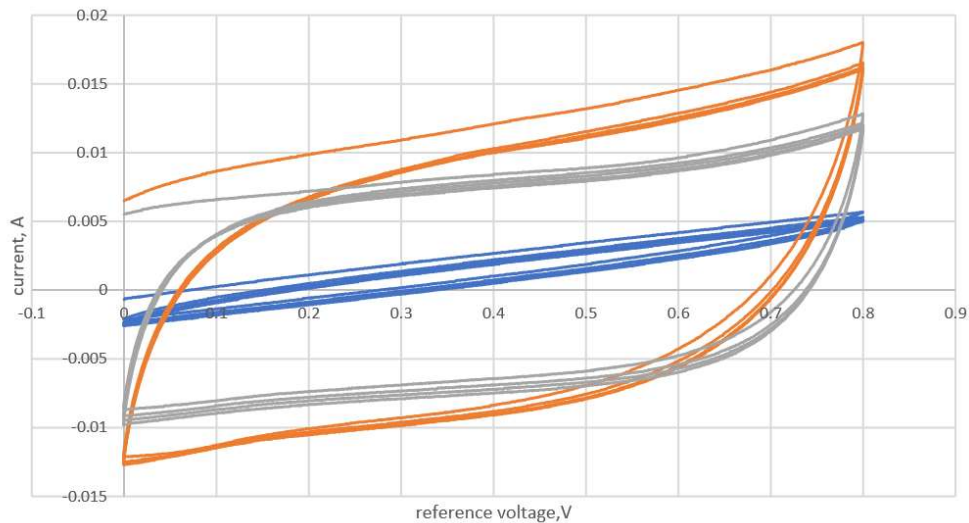


Figure 4.6: The result of CV analysis on silver coated textile EDLC sample 1 (Orange colour line), silver coated textile EDLC sample 2 (grey colour line) and aluminium sheet EDLC sample (blue line).

ITEM	VALUE	Option
Initial delay	<input checked="" type="checkbox"/> Enable	
-Duration(s)	0	
-Stability(V/s)	1.0000e-3	
Deposition	<input type="checkbox"/> Enable	
-Potential(V)	1.0000e+0	Eoc ▼
-Duration(s)	0	
Quiet time(s)	2	
Initial potential(V)	-100.00e-3	ERef ▼
Middle potential(V)	0.0000e+0	ERef ▼
Final potential(V)	800.00e-3	ERef ▼
Scan rate(V/s)	100.00e-3	
Segment count	10	
Sample interval(V)	1.0000e-3	
Limit current(A)	3.0000e+0	
IR Comp.	None ▼	
PF IR(ohm)	0.0000e+0	
I Range(A)	1 A ▼	<input type="checkbox"/> Auto

Figure 4.7: The settings parameter for the CV test.

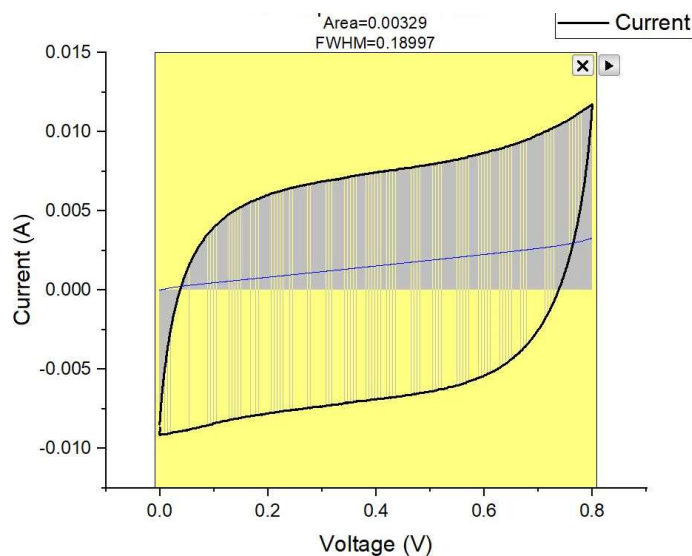


Figure 4.8: Graph plot using OriginPro to calculate the area under the curve.

Based on calculation on all the samples, we can obtain that the areal capacitance of silver coated textile based EDLC is 2.89 mF cm^{-2} , which is higher than the aluminium sheet EDLC sample, which is 0.65 mF cm^{-2} . Furthermore, we can also obtain the specific capacitance of the silver coated textile based EDLC has specific capacitance of 71.32 Fkg^{-1} while the aluminium sheet based EDLC has specific capacitance of 24.78 Fkg^{-1} .

Although the redox reaction peak of both CV curves are clearly shown, but the near ideal EDLC should have near rectangular shape on the CV curve. Only the CV curve of silver coated textile EDLC shows near perfect rectangular shape with larger area compare to the aluminium sheet EDLC. This might be caused by several factors, first, the 3D porous structure of silver coated textile is not the same as planar structure of aluminium sheet EDLC. The 3D porous structure allow better flexibility of the electrodes, more active element, in this case, activated carbon is able to be attached to the surface of the electrodes, which allows the electrodes to store higher amount of energy. Furthermore, compared to the planar structure, which will reduce ion transportation inside the electrodes with thicker material, the 3D porous structure of textile based EDLC doesn't suffer from this situation as the active element is placed inside the 3D porous structure and the ion transportation is the same for both thin and

thick materials (Dong et al., 2016). As the aluminium sheet we use is around 10 micrometer, so it suffers badly from this factor.

A research shows that the commercial silver coated textile EDLC with PVA as electrolyte shows areal capacitance of 46.88 mFcm^{-2} (Pullanchiyodan, Manjakkal, Dervin, Shakthivel & Dahiya, 2020). Another research also shows that a conductive textile substrate electrode made by growing Ni(OH)_2 on ZnO nanowire on textile material shows specific capacitance of 3150 Fg^{-1} (Shakir, Ali, Bae, Park & Kang, 2014). When compared with low areal capacitance achieved by this research's silver coated textile supercapacitor, which is 2.89 mFcm^{-2} and 0.07132 Fg^{-1} . The low capacitance is caused by several errors in the experiment.

First, the activated carbon coating is not brushed evenly on the surface of the electrode, which the actual area to store the ion during charge should be lower than expected and the mass of the active element should be much smaller than the actual measured value. Furthermore, the activated carbon paste brushed on the surface of the electrodes is not very adhesive. During handling of the electrodes, some of the activated carbon powder fall off from the surface of the electrodes, for example, during bending and pressing on the electrode.

Second, the solid-state gel has some pores on it when dried, which causes uneven distribution of the electrolyte across the electrode, where some place is thicker than the other and some place has no contact to the activated carbon, which will hinder the ion transportation of EDLC. Third, the gel is left for 1 week before testing, this might result in oxidation and contamination on the electrolyte, which results in lower ionic transportation rate and causes lower performance on the actual EDLC. Forth, the electrolyte used is not doped with other chemicals like NH_4Br (Mazuki, Abdul Majeed & Samsudin, 2020). Such composition results in lower ionic transportation rate as there are not so many freely moving electron for charge and discharge.

Using the areal capacitance calculated, we can calculate the energy density using the Equation 4.4,

$$E = \frac{1}{2} C_A (\Delta V)^2 \quad (4.4)$$

Where

E = Energy density, W/m^2

C_A = Areal capacitance, $mFcm^{-2}$

ΔV = Potential windows, V

Using this formula, we obtain the energy density of the silver cloth based EDLC as $0.01247 Whcm^{-2}$, while aluminium sample only achieves $0.00117 Whcm^{-2}$, which shows that the silver cloth coated with activated carbon offer bigger surface area to store more energy, while aluminium has a low friction surface which activated carbon is not easily stick to it and reduce the actual surface area for the activated carbon to store energy. Hence, silver clothing is more superior to aluminium in term of energy storage. However, when compare to other EDLC

After that, we can calculate the power density of the EDLC using Equation 4.5,

$$P_A = \frac{(\Delta V)^2}{4AES} \quad (4.5)$$

where

P_A = Power density, W/m^2

A = Area of the active element on EDLC, m^2

ESR = Equivalent series resistance of the supercapacitor, Ω

ΔV = Potential windows, V

The ESR value can be obtained using EIS analysis on the EDLCs, the ESR value is calculated by using Zview as shown in Figure 4.9. Based on the formula, we obtain the power density of the silver cloth based EDLC is $0.01316 Wcm^{-2}$, while aluminium is only generating $0.0031 Wcm^{-2}$. We can conclude that the silver coated textile EDLC shows better power density compare to aluminium sheet EDLC. The results are caused by higher conductivity of silver coated textile and less prone to oxidation during carbon paste coating process compared to aluminium sheet. The silver has electric conductivity of 62.1×10^6 Siemens m^{-1} while aluminium sheet only has 36.9×10^6 Siemens m^{-1} , higher resistivity of aluminium sheet compares to silver coated textile results in lower power density (Jean Tiberghien, 2021).

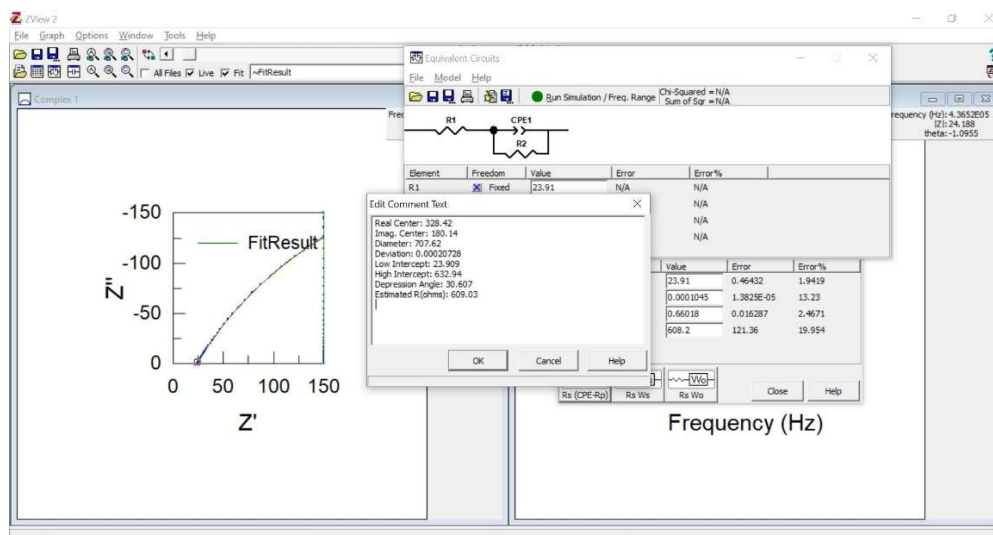


Figure 4.9: Photo illustrates Zview analyse the EIS graph for ESR.

4.5 GCD test on the EDLCs

GCD analysis is conducted based on the setting as shown in Figure 4.10, where the EDLC is constantly charged for 5 seconds and discharged for 5 seconds, and the test run for 100 cycles. The EDLC is charged for 5 seconds only because the EDLC can be fully charged within 5 seconds. Based on the result shown in Figure 4.11, the performance of silver cloth based EDLC has no clear deterioration over 100 cycles after first few cycles, which the EDLC is stabilizing itself. During the first 5 cycles, which the voltage can be charged to 0.8 V for silver coated textile and 0.4 V for aluminium sheet EDLC. However, the first few cycles are ignored as the EDLC is often unstable at the first few cycles and only stabilized after certain amounts of cycles (Sridhar, 2014). As there are no device damage from the first 10 cycles after stabilizes to the last 10 cycles during the 100 cycles, it is predicted that it can perform for 100 cycles more without any problem. Based on the data obtained, GCD should have no negative charge value, but the result shows negatively charged value, this is due to wrong settings for the GCD test, where the EDLC is both positively charged and negatively charged in a time period.

ITEM	VALUE	Option
Charge		
-Const. charge	100.00e-3	Current
-Charging time(s)	5	<input checked="" type="checkbox"/> Enable
-Limit Q (Ah)	360.00e+0	<input type="checkbox"/> Enable
-Limit voltage(V)	3.0000e+0	<input checked="" type="checkbox"/> Enable
-Limit -dV	1.0000e+0	<input checked="" type="checkbox"/> Enable
-Limit temp.	100.00e+0	<input type="checkbox"/> Enable
-Rest time(s)	2	<input checked="" type="checkbox"/> Enable
Discharge		
-Const. discharge	100.00e-3	Current
-Discharging time(s)	5	<input checked="" type="checkbox"/> Enable
-Limit Q (Ah)	0.0000e+0	<input type="checkbox"/> Enable
-Limit voltage(V)	3.0000e+0	<input checked="" type="checkbox"/> Enable
-Rest time(s)	2	<input checked="" type="checkbox"/> Enable
Cycle	100	
Sampling		
-Time(s)	5	<input checked="" type="checkbox"/> Enable
-Delta voltage	1.0000e-3	<input checked="" type="checkbox"/> Enable
-Delta current	1.0000e-3	<input type="checkbox"/> Enable
IR Measure	<input type="checkbox"/> On	
I Range(A)	1 A	<input checked="" type="checkbox"/> Auto

Figure 4.10: Setting for GCD test.

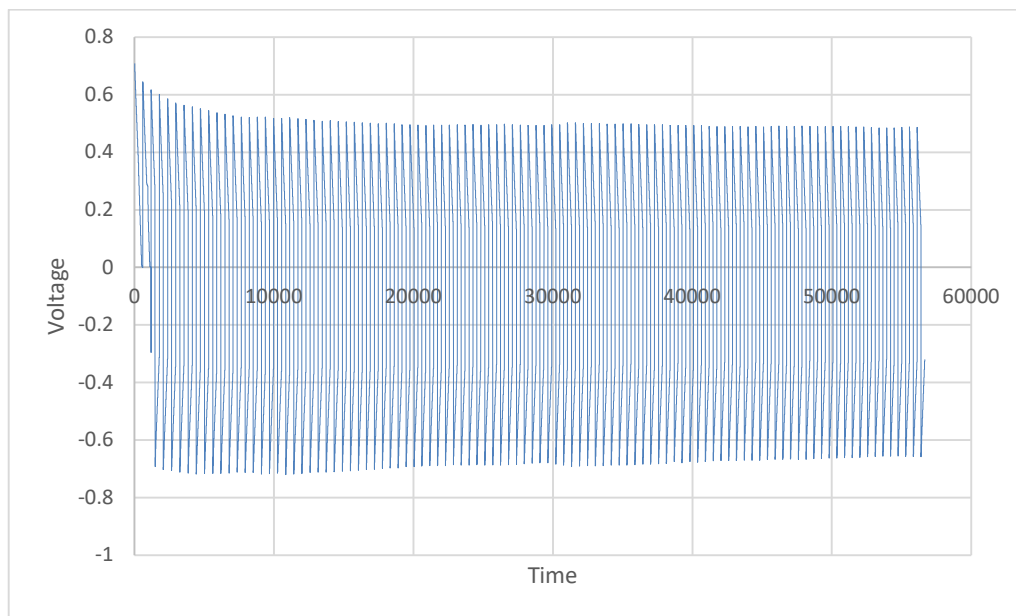


Figure 4.11: GCD testing on silver cloth EDLC (sample 1).

4.6 Output of flexible solar PV

The performance of the flexible solar PV under low light condition and high light condition is recorded. Under low light condition, the solar PV is put under room with no direct sunlight shines on the solar PV, the only available light source is mixed room

LED lightnings. Low light condition has lightning of approximately 100 Wm^{-2} (Apostolou, Reinders & Verwaal, 2016). Based on the result, under low light condition, the flexible solar PV performs badly, which is far from the power output provided by the manufacturer. The solar PV is also put under high light condition, where the solar PV is put under the sun. High light condition has lightning of approximately 1000 Wm^{-2} . The results are tabulated in Figure 4.12.

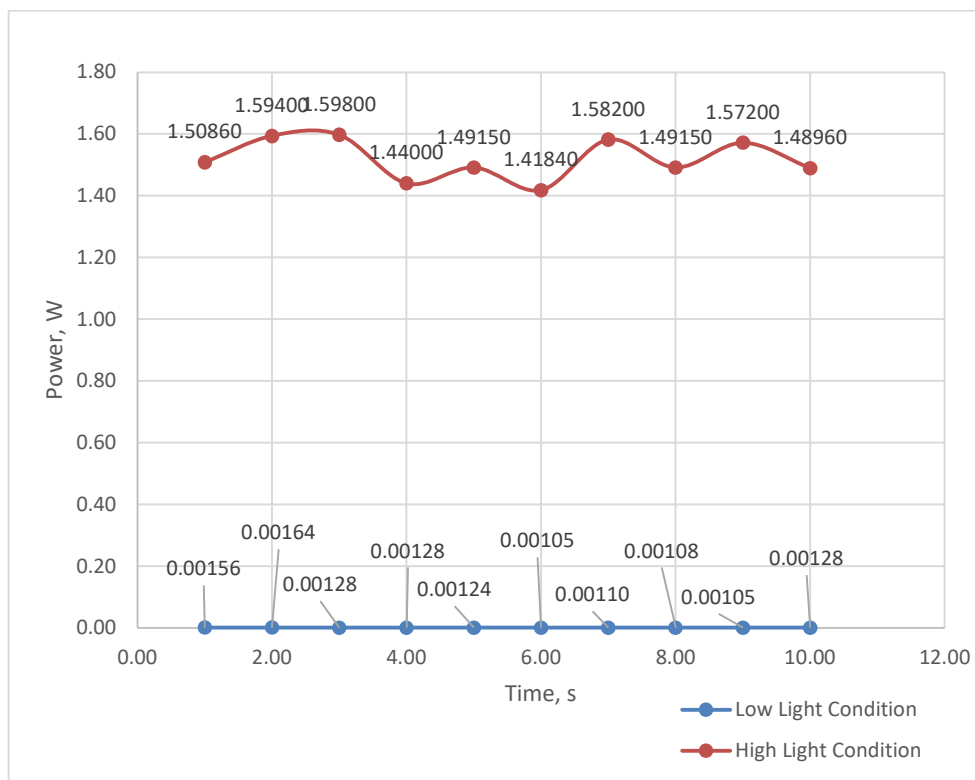


Figure 4.12: Performance of Solar PV under high light and low light condition

Based on the results recorded, the solar PV can averagely output 0.00126 J/s under low light condition and 1.52 J/s under high light condition. The result of the solar PV will provide predicted power to the EDLC under the similar condition, where during high light condition, the solar PV will charge up the EDLC while during low light condition, the power will be too less to generate usable electricity. So, the result of the hybrid solar PV with flexible EDLC under high light condition is recorded only.

4.7 Performance of the hybrid device

To study the performance of integrated hybrid flexible solar PV with flexible EDLC system, the overall energy conversion efficiency, $\eta_{overall}$ is studied. As $\eta_{overall}$ indicates the proportion of the output of the system with the input of the system, the output is measured by the electrical energy output by the EDLC and the input will be the total solar energy input to the solar PV. The equation is represented by Equation 4.6.

$$\eta_{overall} = \frac{I_{dis} \int v dt}{PSt} \quad (4.6)$$

where

I_{dis} = Current discharged by the EDLC, A

$\int v dt$ = Voltage during discharge, V

S = Active light collection area of the solar PV, m²

t = time the light illuminates on the solar PV, s

P = power density of the light receives by the solar PV, W

By calculation, the overall efficiency of the integrated system is 2.2%. It has lower efficiency than integrated system with solar PV, supercapacitor and battery, which has overall efficiency of 5% and above. One study that uses hierarchical NiCo₂O₄ battery-supercapacitor hybrid shows overall efficiency of 8.1%. The low efficiency of such integrated system is caused by the lack of use of battery in the system, which result in unstable current and voltage discharge and result in total lower power output.

Based on the experiment conducted, the data is plotted in Figure 4.13. When the silver coated EDLC is charged by direct sunlight provided by a solar PV for 5 seconds, the silver cloth EDLC can continuously discharge electricity for 1 hour before it becomes 0.3V and 12 minutes and 8 seconds for it to turns from 3.3V to 1.8V, which is the forward voltage of a normal 5mm LED bulb. The higher power density of silver coated textile EDLC causes the greater amount of energy releases to the circuit in a shorter time. Hence, when compare to aluminium sheet EDLC, which uses 18 minutes to releases electricity with voltage from 3.3V to 1.8V, the lower power density allows the aluminium sheet EDLC to power the wearable electronics for longer period. By using supercapacitor power management module with the silver coated textile EDLC,

it is expected that silver coated textile EDLC can output electricity for a longer period and power up wearable electronics for a longer time (Brooks et al, 2014).

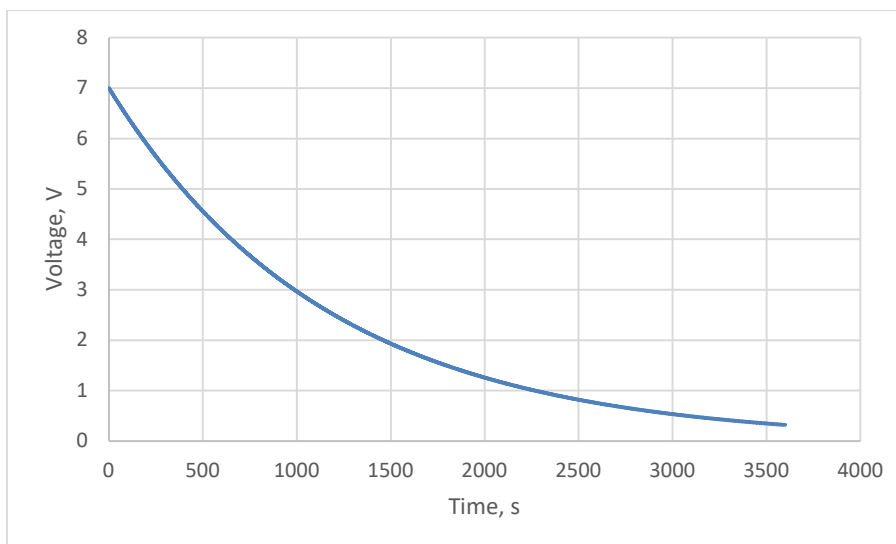


Figure 4.13: Graph of output of voltage over time for silver coated textile EDLC

But with the fast charge rate with only 5 seconds and slow discharge rate provided by the silver cloth EDLC, which takes total 27 minutes to discharge from 7 V to 1.8 V, it is able to pair with a battery or any material with higher energy storage capacity material to continuously charge the energy storage material for usage throughout the day and night. This is because based on the result recorded, the integrated device consisting of supercapacitor and solar PV can only effectively power up electronics for up to 30 minutes.

4.8 Summary

Based on the experiment result, the EDLC made of silver textile has a fast-charging rate, capable of storing enough energy to provide a normal electronic enough electricity to power wearable electronics for 30 minutes. When paired with battery, it provides continuous electricity output to the battery, which solve the inconsistency of solar PV electricity output. As the EDLC uses 1 hour to release the voltage until 0.3 V, by further increasing the amount of EDLC used, we can store enough energy to power up electronics for 1 hour or more without problem. Furthermore, the lightweight of EDLC and solar PV is suitable to be knitted together to form a standalone power generating device with smoother discharge rate, and be able to supply electricity

throughout the day, while battery will be needed to provide 24 hours electricity supply, as the energy density provided by silver textile EDLC, which is only $0.00325 \text{ Whcm}^{-2}$, is considered low compared to battery.

CHAPTER 5

CONCLUSIONS AND RECOMMENDATIONS

5.1 Conclusions

In this project, we have proposed a hybrid flexible solar PV with EDLC made of silver coated textile. The solid-state electrolyte, PVA and H₃PO₄ gel, used for making the EDLCs show ionic conductivity of 0.00002954 S/m and voltage windows of 1.5 V. The silver coated textile EDLC used in the device shows an areal capacitance of 2.89 mFcm⁻², specific capacitance of 71.32 Fkg⁻¹, energy density of 0.01247 Whcm⁻², power density of 0.01316 Wcm⁻², prolonged cycling stability, which hits 100% retention rate after 100 cycles. Furthermore, when the EDLC is paired with flexible solar PV to form a standalone power generating and storing device, it achieves overall conversion efficiency of 2.2%. The 25 cm² of EDLC is able to supply sufficient power to power up the wearable electronics for 30 minutes with 5 seconds of charging.

In short, the test results show that the flexible EDLC with flexible solar PV is workable under the sun and daily outdoor activity to ensure continuous electricity supply. It can store enough energy for a person to move from high light to low light area before the person back to high light area. Both the solar PV and EDLCs made are lightweight, nontoxic and flexible for wearability application. Thus, all the objectives in the project is successfully achieved.

5.2 Recommendations for future work

Based on the result of the project, there are several recommendations for the fabrication of the EDLC and flexible solar PV. Due to limitation of time and resources, many things are unable to be done during this experiment, therefore future works are recommended to get a better result.

First, the solar PV should be fabricated with textile material, or any material with similar flexibility as silver cloth, as this will allow both materials to be easily knitted together and still have a similar flexibility. When knitted, the wire can be fixed easily, the whole device can be carried around easier and more accurate testing result for the standalone solar PV with EDLC device can be obtained.

Second, the electrolyte used in EDLC should be prepared with different doping material to increase the ion conductivity of the electrolyte and mechanical properties of the electrolyte. This is because without doping material in the electrolyte composition, the electrolyte will have lower energy capacity and power density as the free moving electrons are lesser. The electrolyte should also have the same flexibility and sketchability as the electrode, which is the silver coated textile to make it more flexible.

Third, the adhesion of the activated carbon paste is low, where most of the powder fall off during handling of the EDLC, which result in poor capacitive performance of the aluminium sheet and silver coated textile. Hence, etching should be performed on the surface of aluminium sheet before apply carbon coating, this will greatly increase the adhesion of activated carbon layer, which can get more accurate result on the EDLC made of aluminium sheet electrode. Another formula that has more adhesive properties should be used for the activated carbon paste. Furthermore, the coating method can also be improved, the silver coated textile should be coated with screen print method to get a better coating, where the activated carbon layers thickness is the same at all surface.

Forth, the textile based EDLC should be made with other brand of silver coated cloth to a more optimised result of EDLC made with silver coated textile, as different brand will have different manufacturing method, which will result in different capacitance. The silver coated cloth should be cutting to exact size, which is 25cm^2 in this experiment, using laser cutter instead of scissors to get a more accurate result.

REFERENCES

- 3 generations of solar cells: solar facts and advice. (2020). Retrieved 27 August 2020, from <https://www.solar-facts-and-advice.com/solar-cells.html>
- Alipoori, S., Mazinani, S., Aboutalebi, S., & Sharif, F. (2020). Review of PVA-based gel polymer electrolytes in flexible solid-state supercapacitors: Opportunities and challenges. *Journal Of Energy Storage*, 27, 101072. <https://doi.org/10.1016/j.est.2019.101072>
- Apostolou, G., Reinders, A., & Verwaal, M. (2016). Comparison of the indoor performance of 12 commercial PV products by a simple model. *Energy Science & Engineering*, 4(1), 69-85. doi: 10.1002/ese3.110
- Brooks., Michael, F., Anderson., & Kehoe, B. (2014). Supercapacitor power management module. *Electrical Engineering Senior*. Retrieved 27 August 2020, from https://scholarcommons.scu.edu/cgi/viewcontent.cgi?article=1006&context=elec_senior
- Brza, M., B. Aziz, S., Anuar, H., Dannoun, E., Ali, F., & Abdulwahid, R. et al. (2020). The study of EDLC device with high electrochemical performance fabricated from proton ion conducting PVA-Based polymer composite electrolytes plasticized with glycerol. *polymers*, 12(9), 1896. doi: 10.3390/polym12091896
- Cyclic voltammetry, EIS, leakage current-testing electrochemical capacitors. (2020). Retrieved 2 September 2020, from <https://www.gamry.com/application-notes/battery-research/testing-electrochemical-capacitors-cyclic-voltammetry-leakage-current/>
- Dong, L., Xu, C., Li, Y., Huang, Z., Kang, F., Yang, Q., & Zhao, X. (2016). Flexible electrodes and supercapacitors for wearable energy storage: a review by category. *Journal Of Materials Chemistry A*, 4(13), 4659-4685. doi: 10.1039/c5ta10582j
- Dubal, D., Kim, J., Kim, Y., Holze, R., & Kim, W. (2013). Demonstrating the highest supercapacitive performance of branched MnO₂ Nanorods grown directly on flexible substrates using controlled chemistry at ambient temperature. *Energy Technology*, 1(2-3), 125-130. doi: 10.1002/ente.201200040
- Dunne, L. (2015). Wearable technology. Retrieved 6 September 2020, from <https://www.britannica.com/topic/Wearable-Technology-2008498>
- Field, H. (2017). Methods and instruments for the characterization of solar cells. *Photovoltaic Solar Energy*, 303-321. doi: 10.1002/9781118927496.ch29

Fu, Q., Tang, X., Huang, B., Hu, T., Tan, L., Chen, L., & Chen, Y. (2018). Recent Progress on the long-term stability of perovskite solar cells. *Advanced Science*, 5(5), 1700387. doi: 10.1002/advs.201700387

Fu, Y., Cai, X., Wu, H., Lv, Z., Hou, S., & Peng, M. et al. (2012). Fiber supercapacitors utilizing pen ink for flexible/wearable energy storage. *Advanced Materials*, 24(42), 5713-5718. doi: 10.1002/adma.201202930

Hashemi, S, A., Ramakrishna, S., & Aberla, A. (2020). Recent progress in flexible-wearable solar cells for self-powered electronic devices. *Energy and Environmental Science*. doi: 10.1039/C9EE03046H.

Heimböckel, R., Hoffmann, F., & Fröba, M. (2019). Insights into the influence of the pore size and surface area of activated carbons on the energy storage of electric double layer capacitors with a new potentially universally applicable capacitor model. *Physical Chemistry Chemical Physics*, 21(6), 3122-3133. doi: 10.1039/c8cp06443a

Hösel, M., Angmo, D., & Krebs, F. (2013). Organic solar cells (OSCs). *Handbook Of Organic Materials For Optical And (Opto)Electronic Devices*, 473-507. doi: 10.1533/9780857098764.3.473

Hu, L., Choi, J., Yang, Y., Jeong, S., La Mantia, F., Cui, L., & Cui, Y. (2009). Highly conductive paper for energy-storage devices. *Proceedings Of The National Academy Of Sciences*, 106(51), 21490-21494. doi: 10.1073/pnas.0908858106

Hu, L., Pasta, M., La Mantia, F., Cui, L., Jeong, S., & Deshazer, H. et al. (2010). Stretchable, Porous, and Conductive Energy Textiles. *Nano Letters*, 10(2), 708-714. doi: 10.1021/nl903949m

Hu, S., Rajamani, R., & Yu, X. (2012). Flexible solid-state paper based carbon nanotube supercapacitor. *Applied Physics Letters*, 100(10), 104103. doi: 10.1063/1.3691948

Jean Tiberghien, G. (2021). TIBTECH innovations: metal properties comparison: electric conductivity, thermal conductivity, density, melting temperature. Retrieved 6 April 2021, from https://www.tibtech.com/conductivite.php?lang=en_US

Josef, E., Yan, R., Guterman, R., & Oschatz, M. (2019). Electrospun carbon fibers replace metals as a current collector in supercapacitors. *ACS Applied Energy Materials*, 2(8), 5724-5733. doi: 10.1021/acsaem.9b00854

Jost, K., Dion, G., & Gogotsi, Y. (2014). Textile energy storage in perspective. *Journal Of Materials Chemistry A*, 2(28), 10776. doi: 10.1039/c4ta00203b

Kalia, T. (2020). 6 key challenges of wearable product development. Retrieved 6 September 2020, from <https://medium.com/@outdesign/6-key-challenges-of->

wearable-product-development-49717d88c684#:~:text=Security%20and%20Privacy%20concerns%20of,of%20encryption%20and%20other%20vulnerabilities.

Largeot, C., Portet, C., Chmiola, J., Taberna, P., Gogotsi, Y., & Simon, P. (2008). Relation between the Ion Size and Pore Size for an Electric Double-Layer Capacitor. *Journal Of The American Chemical Society*, 130(9), 2730-2731. doi: 10.1021/ja7106178

Li, L., Wu, Z., Yuan, S., & Zhang, X. (2014). Advances and challenges for flexible energy storage and conversion devices and systems. *Energy & Environmental Science*, 7(7), 2101. doi: 10.1039/c4ee00318g

Li, W., Mak, C., Kan, C., & Hui, C. (2014). Enhancing the capacitive performance of a textile-based CNT supercapacitor. *RSC Adv.*, 4(110), 64890-64900. doi: 10.1039/c4ra10450a

Lin, Y., Chen, J., Tavakoli, M., Gao, Y., Zhu, Y., & Zhang, D. et al. (2018). Printable fabrication of a fully integrated and self-powered sensor system on plastic substrates. *Advanced Materials*, 31(5), 1804285. doi: 10.1002/adma.201804285

Liu, R., Wang, J., Sun, T., Wang, M., Wu, C., & Zou, H. et al. (2017). Silicon nanowire/polymer hybrid solar cell-supercapacitor: a self-charging power unit with a total efficiency of 10.5%. *Nano Letters*, 17(7), 4240-4247. doi: 10.1021/acs.nanolett.7b01154

Manjakkal, L., Núñez, C., Dang, W., & Dahiya, R. (2018). Flexible self-charging supercapacitor based on graphene-Ag-3D graphene foam electrodes. *Nano Energy*, 51, 604-612. doi: 10.1016/j.nanoen.2018.06.072

Mazuki, N., Abdul Majeed, A., & Samsudin, A. (2020). Study on electrochemical properties of CMC-PVA doped NH₄Br based solid polymer electrolytes system as application for EDLC. *Journal Of Polymer Research*, 27(6). doi: 10.1007/s10965-020-02078-5

Melkiyur, I. (2020). Re: how can I calculate the energy density and power density?. Retrieved from: <https://www.researchgate.net/post/How-can-I-calculate-the-energy-density-and-power-density/5efcd72db24a04313e4fd246/citation/download>.

Meng, C., Liu, C., Chen, L., Hu, C., & Fan, S. (2010). Highly flexible and all-solid-state paperlike polymer supercapacitors. *Nano Letters*, 10(10), 4025-4031. doi: 10.1021/nl1019672

Moazami, H. (2017). Re: What is the relation between capacitance and conductance?. Retrieved from: https://www.researchgate.net/post/What_is_the_relation_between_capacitance_and_conductance/59d0eef9f7b67e15c048fac2/citation/download.

Mozaffari, S., Nateghi, M., & Zarandi, M. (2017). An overview of the challenges in the commercialization of dye sensitized solar cells. *Renewable And Sustainable Energy Reviews*, 71, 675-686. doi: 10.1016/j.rser.2016.12.096

Murata electronics. (2020). High performance electrical double-layer capacitors. Retrieved 27 August 2020, from https://www.mouser.com/pdfDocs/Murata-DMF-DMT_TechnicalGuide.pdf

Ng, C., Lim, H., Hayase, S., Harrison, I., Pandikumar, A., & Huang, N. (2015). Potential active materials for photo-supercapacitor: A review. *Journal Of Power Sources*, 296, 169-185. doi: 10.1016/j.jpowsour.2015.07.006

Pratap Kharwar, Y. (2016). Re: I want to calculate capacitance from CV data. Can anybody please tell me which value of potential I have to take for making the calculations?. Retrieved 29 August 2020 from: <https://www.researchgate.net/post/I-want-to-calculate-capacitance-from-CV-data-Can-anybody-please-tell-me-which-value-of-potential-I-have-to-take-for-making-the-calculations/573eddc5ed99e10c82202fd6/citation/download>.

Pullanchiyodan, A., Manjakkal, L., Dervin, S., Shakthivel, D. and Dahiya, R. (2020). Metal Coated Conductive Fabrics with Graphite Electrodes and Biocompatible Gel Electrolyte for Wearable Supercapacitors. *Advanced Materials Technologies*, 5(5), p.1901107.

Pullanchiyodan, A., Manjakkal, L., Dervin, S., Shakthivel, D., & Dahiya, R. (2020). Metal Coated Conductive Fabrics with Graphite Electrodes and Biocompatible Gel Electrolyte for Wearable Supercapacitors. *Advanced Materials Technologies*, 5(5), 1901107. doi: 10.1002/admt.201901107

Ruther, R., Sun, C., Holliday, A., Cheng, S., Delnick, F., Zawodzinski, T., & Nanda, J. (2016). Stable Electrolyte for High Voltage Electrochemical Double-Layer Capacitors. *Journal Of The Electrochemical Society*, 164(2), A277-A283. doi: 10.1149/2.0951702jes

Sakurai, M., & Sakai, T. (1999). Current status and future trends of amorphous silicone solar cells. Retrieved 25 March 2021, from <https://www.fujielectric.com/company/tech/pdf/r52-3/03.pdf>

Sharma, K., Sharma, V., & Sharma, S. (2018). Dye-Sensitized solar cells: fundamentals and current status. *Nanoscale Research Letters*, 13(1). doi: 10.1186/s11671-018-2760-6

Sheberla, D., Bachman, J., Elias, J., Sun, C., Shao-Horn, Y., & Dincă, M. (2016). Conductive MOF electrodes for stable supercapacitors with high areal capacitance. *Nature Materials*, 16(2), 220-224. doi: 10.1038/nmat4766

Sridhar, D. (2014). Re: how might one measure capacitance retention from charging-discharging profile of a supercapacitor?. Retrieved from: https://www.researchgate.net/post/How_might_one_measure_capacitance_retention_from_charging-discharging_profile_of_a_supercapacitor/546317bccf57d7016b8b468f/citation/download.

Stoller, M., Park, S., Zhu, Y., An, J., & Ruoff, R. (2008). Graphene-based ultracapacitors. *Nano Letters*, 8(10), 3498-3502. doi: 10.1021/nl802558y

Tang, Y., Li, X., Lv, H., Wang, W., Zhi, C., & Li, H. (2020). Integration designs toward new - generation wearable energy supply - sensor systems for real - time health monitoring: A minireview. *Infomat*. doi: 10.1002/inf2.12102

Tian, J., Cui, C., Xie, Q., Qian, W., Xue, C., & Miao, Y. et al. (2018). EMIMBF4–GBL binary electrolyte working at -70°C and 3.7 V for a high performance graphene-based capacitor. *Journal Of Materials Chemistry A*, 6(8), 3593-3601. doi: 10.1039/c7ta10474j

Vivek, K. (2014). Organic solar cells: principles, mechanism and recent developments. *International Journal Of Research In Engineering And Technology*, 03(09), 338-341. doi: 10.15623/ijret.2014.0309053

Wu, Y., & Cao, C. (2018). The way to improve the energy density of supercapacitors: Progress and perspective. *Science China Materials*, 61(12), 1517-1526. doi: 10.1007/s40843-018-9290-y

Yang, C., Hsu, S., & Chien, W. (2005). All solid-state electric double-layer capacitors based on alkaline polyvinyl alcohol polymer electrolytes. *Journal Of Power Sources*, 152, 303-310. doi: 10.1016/j.jpowsour.2005.03.004

Yu, M., & Feng, X. (2019). Thin-film electrode-based supercapacitors. *Joule*, 3(2), 338-360. doi: 10.1016/j.joule.2018.12.012

Yu, N., Yin, H., Zhang, W., Liu, Y., Tang, Z., & Zhu, M. (2015). High-performance fiber-shaped all-solid-state asymmetric supercapacitors based on ultrathin MnO₂Nanosheet / carbon fiber cathodes for wearable electronics. *Advanced Energy Materials*, 6(2), 1501458. doi: 10.1002/aenm.201501458

Yuan, Y., Lu, Y., Jia, B., Tang, H., Chen, L., & Zeng, Y. et al. (2019). Integrated system of solar cells with hierarchical NiCo₂O₄ battery-supercapacitor hybrid devices for self-driving light-emitting diodes. *Nano-Micro Letters*, 11(1). doi: 10.1007/s40820-019-0274-0

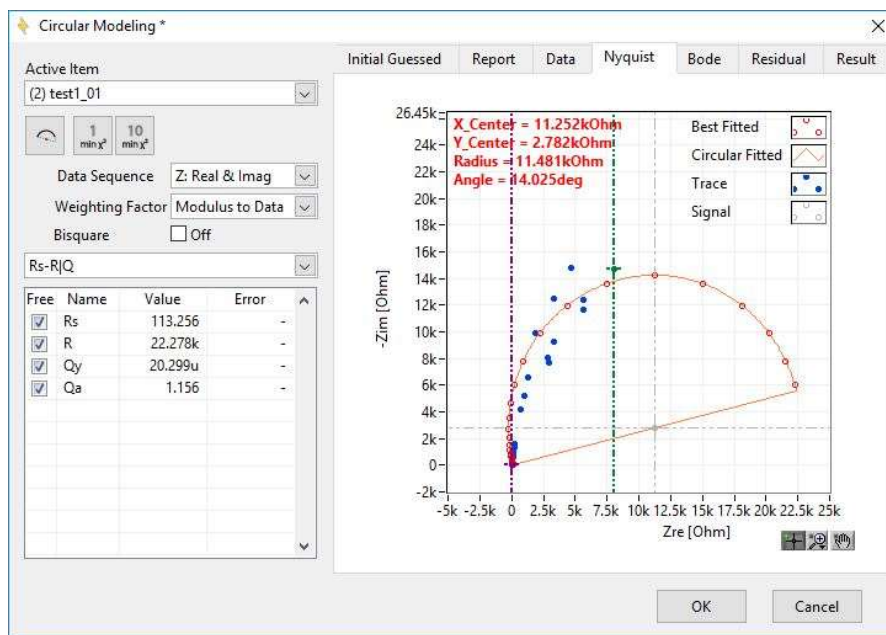
Zhai, S., Karahan, H. E., Wei, L., Qian, Q., Harris, A. T., Minett, A. I., Chen, Y. (2016). Textile energy storage: structural design concepts, material selection and future perspectives. *Energy Storage Materials*, 3, 123–139. doi:10.1016/j.ensm.2016.02.003

Zhang, C., Song, Y., Wang, M., Yin, M., Zhu, X., & Tian, L. et al. (2017). Efficient and flexible thin film amorphous silicon solar cells on nanotextured polymer substrate using sol-gel based nanoimprinting method. *Advanced Functional Materials*, 27(13), 1604720. doi: 10.1002/adfm.201604720

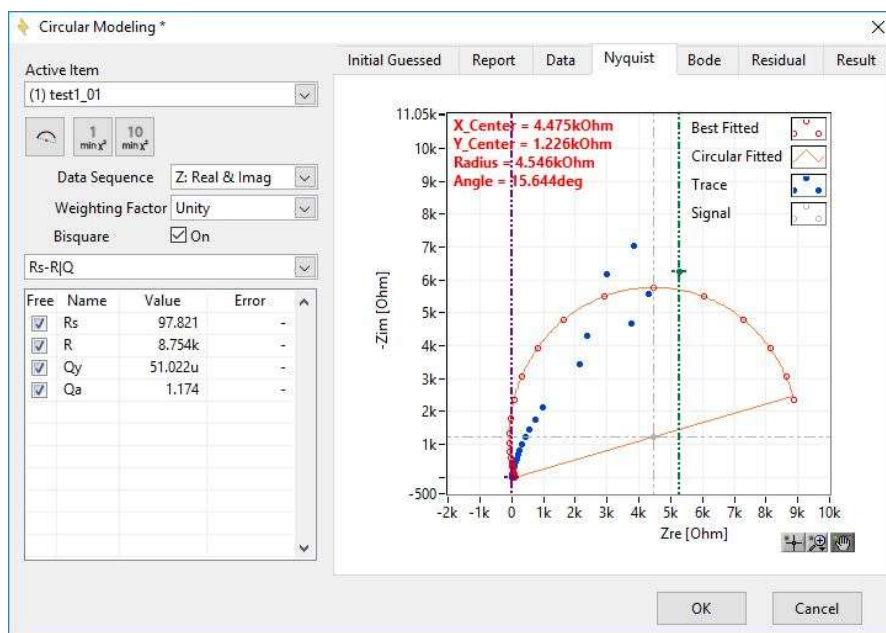
Zhang, M., He, L., Shi, T., & Zha, R. (2018). Nanocasting and direct synthesis strategies for mesoporous carbons as supercapacitor electrodes. *Chemistry Of Materials*, 30(21), 7391-7412. doi: 10.1021/acs.chemmater.8b03345

APPENDICES

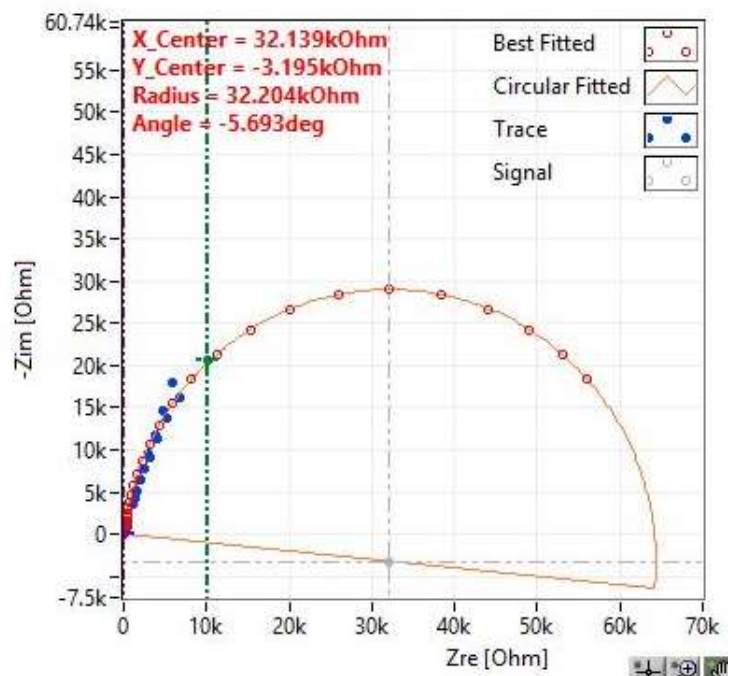
APPENDIX A: Circular modelling of nyquist plot data using ZMAN Zive



(a) PVA Gel sample 1

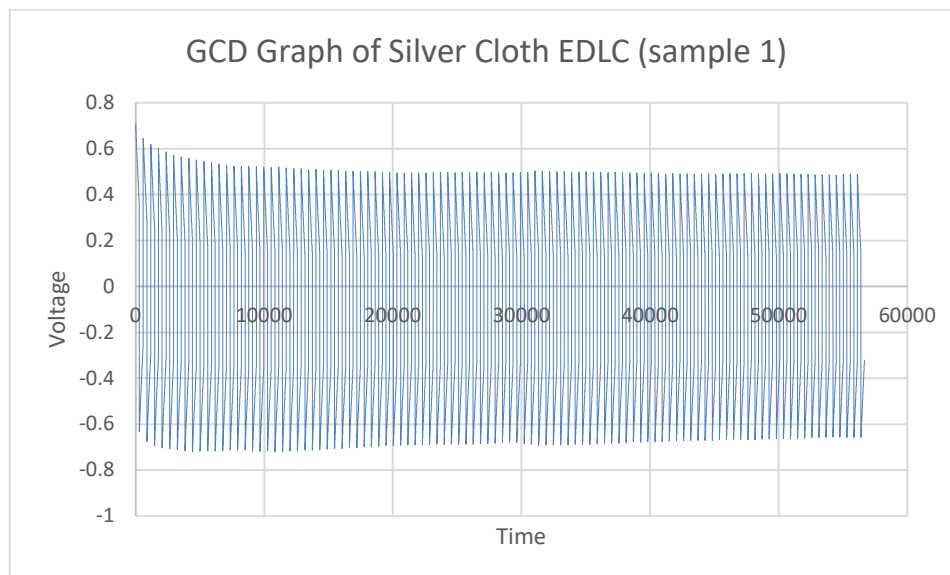


(b) PVA gel sample 2

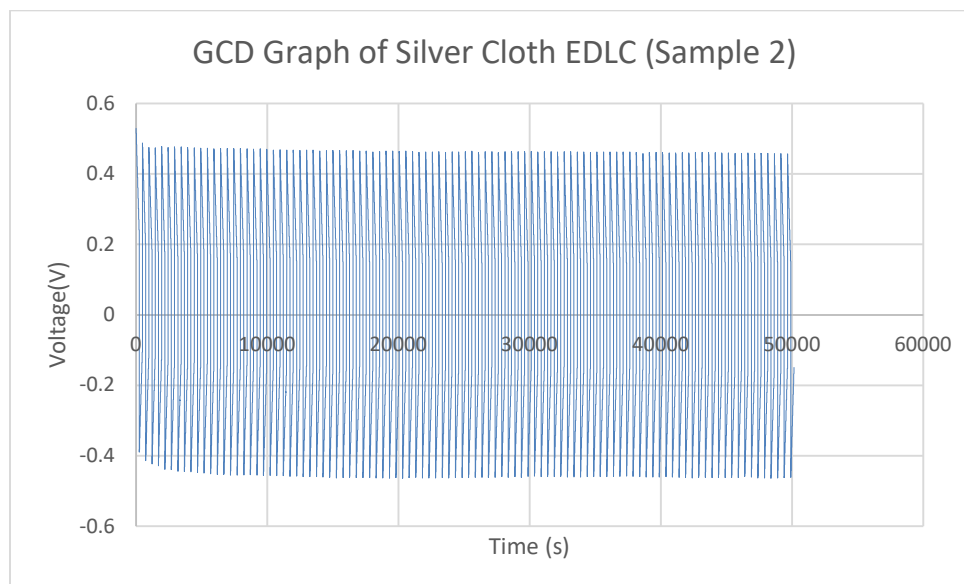


(c) PVA gel sample 3

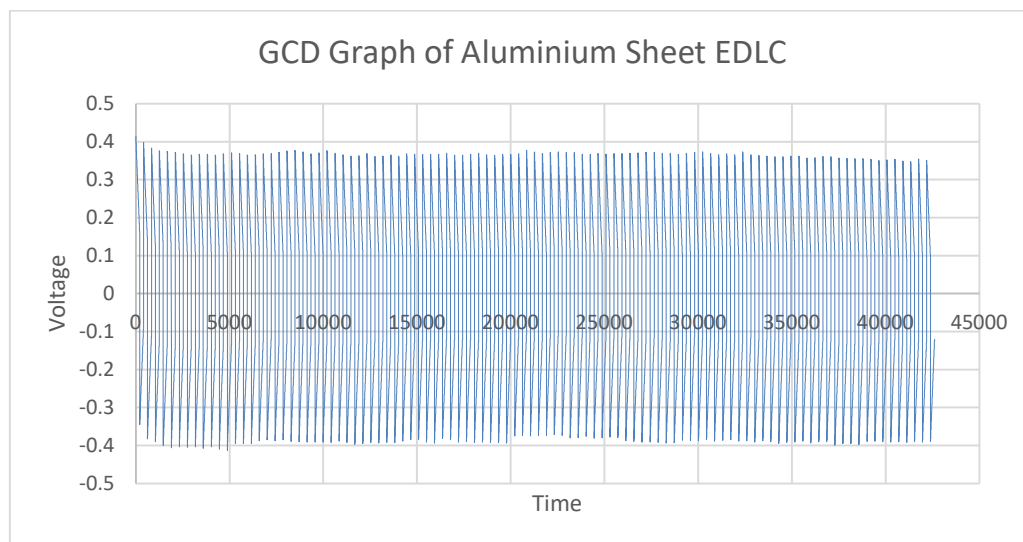
APPENDIX B: GCD Graph of EDLCs



(a) GCD Graph of Silver Cloth EDLC (Sample 1)

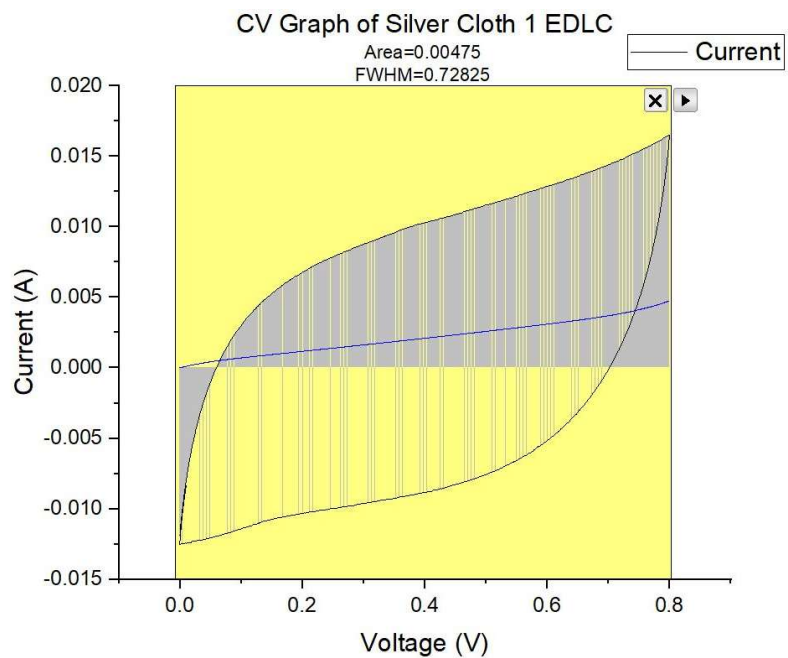


(b) GCD Graph of Silver Cloth EDLC (Sample 2)

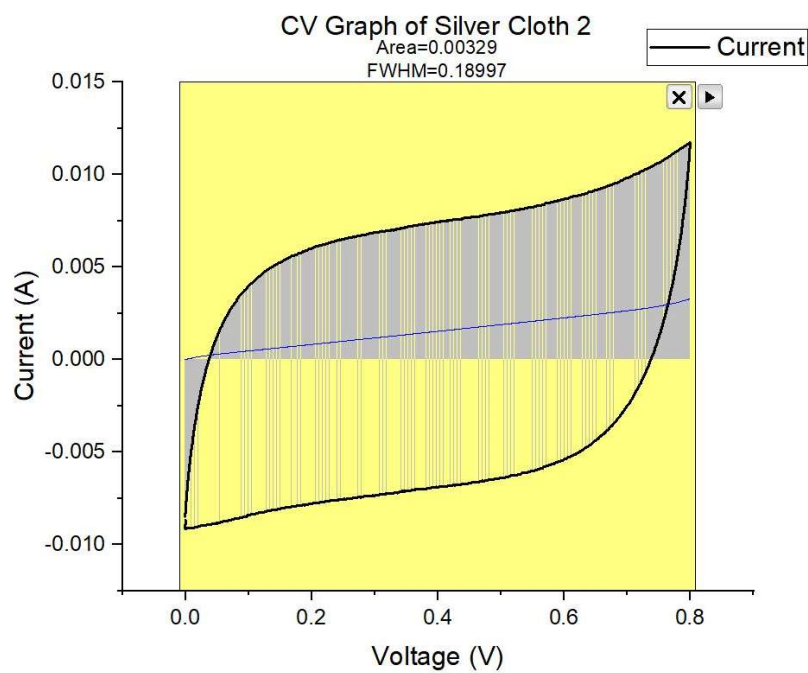


(c) GCD Graph of Aluminum Sheet EDLC

APPENDIX C: CV Graph of EDLCs

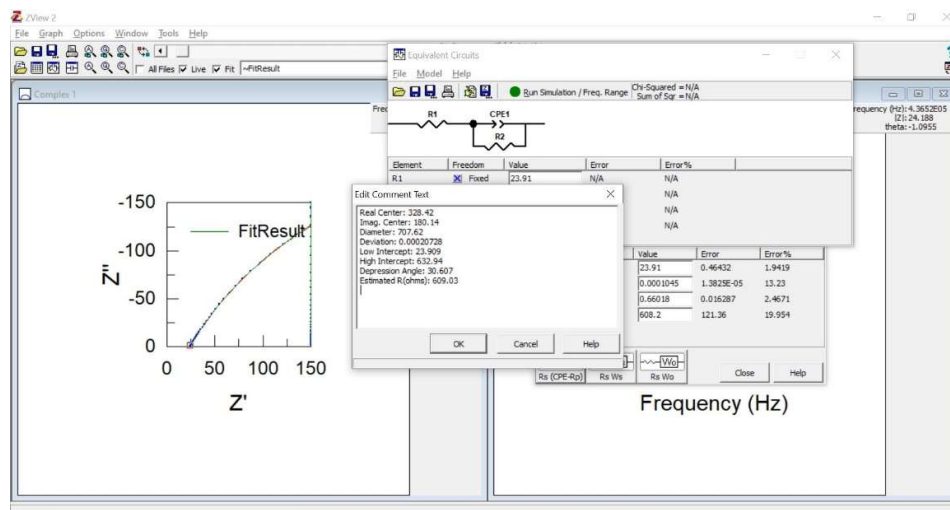


(a) CV Graph of silver coated textile EDLC (Sample 1)

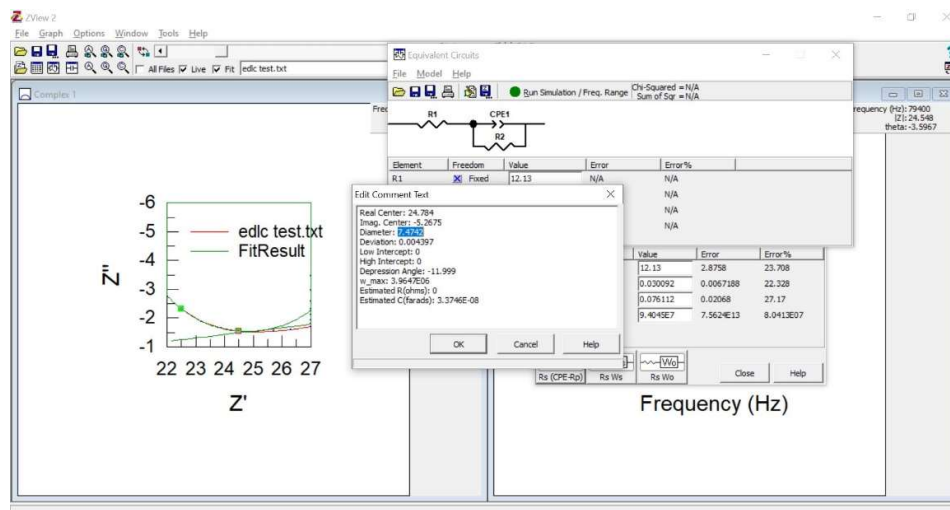


(b) CV Graph of silver coated textile EDLC (Sample 2)

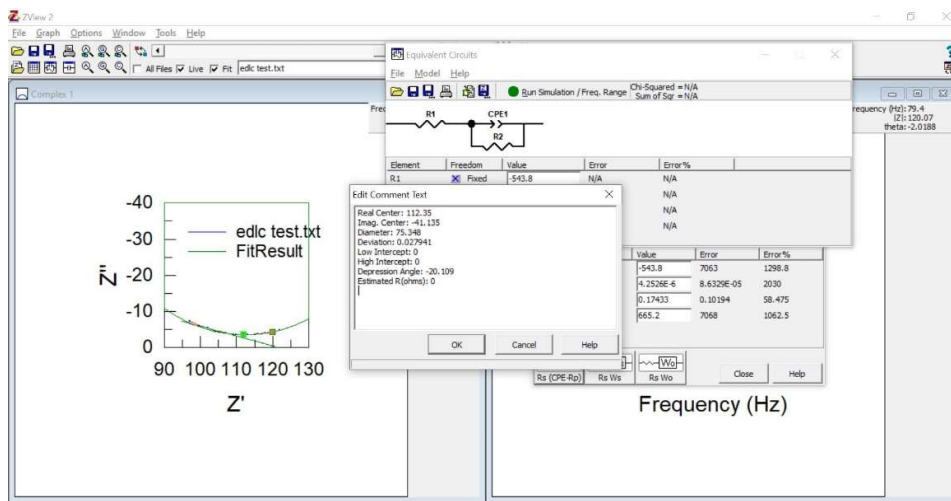
APPENDIX D: Nyquist graph fitting of EDLCs using Zview.



(a) Nyquist graph fitting of silver coated textile EDLC (sample 1)



(b) Nyquist graph fitting of silver coated textile EDLC (sample 2)



(c) Nyquist graph fitting of aluminium sheet EDLC.

APPENDIX E: Calculations

(a) Areal capacitance calculation

$$\begin{aligned}
C_{a(\text{silver cloth sample 1})} &= C_A = \frac{1}{2A\Delta Vv} \int I dV \\
&= \frac{0.00475}{2(5.72)(1.5)(0.1)} = 2.77 \text{ mFcm}^{-2} \\
C_{a(\text{silver cloth sample 2})} &= \frac{1}{2A\Delta Vv} \int I dV = \frac{0.00329}{2(3.8)(1.5)(0.1)} = 2.89 \text{ mFcm}^{-2} \\
C_{a(\text{aluminium sheet sample})} &= \frac{1}{2A\Delta Vv} \int I dV = \frac{0.00165}{2(8.5)(1.5)(0.1)} = 0.65 \text{ mFcm}^{-2}
\end{aligned}$$

(b) Specific capacitance calculation

$$\begin{aligned}
m_{\text{active element}} &= m_{\text{after putting carbon paste}} - m_{\text{before putting carbon paste}} \\
&= 0.467 - 0.245 = 0.222 \text{ g} = 0.000222 \text{ kg} \\
C_{p(\text{silver cloth sample 1})} &= C_p = \frac{\int I dv}{2m\Delta Vv} \\
&= \frac{0.00475}{2(0.000222)(1.5)(0.1)} = 71.32 \text{ Fkg}^{-1} \\
C_{p(\text{silver cloth sample 2})} &= C_p = \frac{\int I dv}{2m\Delta Vv} = \frac{0.00329}{2(0.000222)(1.5)(0.1)} = 49.39 \text{ Fkg}^{-1} \\
C_{p(\text{aluminium sheet sample})} &= C_p = \frac{\int I dv}{2m\Delta Vv} = \frac{0.00165}{2(0.000222)(1.5)(0.1)} \\
&= 24.78 \text{ Fkg}^{-1}
\end{aligned}$$

(c) Energy density calculation

$$\begin{aligned}
E_{(\text{silver cloth sample 1})} &= \frac{1}{2} C_A (\Delta V)^2 \\
&= \frac{1}{2} (0.00277)(1.5)^2 = 0.00312 \text{ Whcm}^{-2} \\
E_{(\text{silver cloth sample 2})} &= \frac{1}{2} C_A (\Delta V)^2 \\
&= \frac{1}{2} (0.00289)(1.5)^2 = 0.00325 \text{ Whcm}^{-2} \\
E_{(\text{aluminium sheet sample})} &= \frac{1}{2} C_A (\Delta V)^2
\end{aligned}$$

$$= \frac{1}{2}(0.00065)(1.5)^2 = 0.000731 \text{ Whcm}^{-2}$$

(d) Power density calculation

$$P_{\text{silver cloth sample 1}} = \frac{(\Delta V)^2}{4AESR}$$

$$= \frac{1.5^2}{4(5.72)(7.474)} = 0.01316 \text{ Wcm}^{-2}$$

$$P_{\text{silver cloth sample 2}} = \frac{(\Delta V)^2}{4AESR}$$

$$= \frac{1.5^2}{4(2.63)(76.98)} = 0.0028 \text{ Wcm}^{-2}$$

$$P_{\text{aluminium sample 1}} = \frac{(\Delta V)^2}{4AESR}$$

$$= \frac{1.5^2}{4(0.26)(707.62)} = 0.0031 \text{ Wcm}^{-2}$$

(e) Overall efficiency calculation

$$\eta_{\text{overall}} = \frac{I_{\text{dis}} \int v dt}{PSt} = \frac{(0.5)(7)}{1000(0.365 \times 0.085)(5)} = 0.022 = 2.2\%$$